OBSERVED PROPERTIES OF INTERSTELLAR DUST

×2146

Blair D. Savage and John S. Mathis

Washburn Observatory, University of Wisconsin, Madison, Wisconsin 53706

Introduction

Interstellar dust plays a significant role in influencing the physical and chemical state of the interstellar medium. It now appears well established that H_2, the most abundant molecule in the interstellar medium, forms on dust grains (Spitzer 1978). The dust contains a significant fraction of the interstellar heavy elements and thereby ties up important atomic species that can cool the interstellar gas through collisionally excited fine structure transitions. The dust, because of its large opacity, influences the diffuse interstellar radiation field and undoubtedly has a fundamental effect on the processes whereby interstellar clouds collapse to form stars. Unfortunately, the obscuring effects of dust can introduce very significant uncertainties in the interpretation of the energy distributions of astronomical sources situated behind dust clouds. Progress in understanding the nature of interstellar dust therefore not only provides important information about a significant constituent of the universe, but also should help observational astronomers to improve their correction procedures for the extinction produced by dust.

This review will concentrate on providing up-to-date information on the observed properties of interstellar dust. An attempt will be made to clarify some of the observational uncertainties associated with obtaining dust parameters. In some cases, our state of understanding is quite advanced, while, in other cases, observational and interpretative difficulties introduce large errors in the inferred parameters. About 300 research papers that are in some way related to cosmic dust are published each year. Obviously, it is impossible in a short review to adequately cover all such work, or to treat interesting side investigations. Some topics omitted include: the alignment of grains (see Spitzer 1978 and Aannestad & Purcell 1973); solar system grains (see McDonnell 1978 and Elsässer & Fechtig 1976); extragalactic dust; and circumstellar dust (see Ney

73

Table 1   Recent review papers or books discussing cosmic dust

Author(s)	Title	Comments
Aannestad & Purcell 1973	Interstellar Grains	Extensive review of interstellar dust
Andriesse 1977	Radiating Cosmic Dust	Theoretically oriented review
de Jong 1976	Interstellar Dust: Invited Review	General review of interstellar dust
Elsässer & Fechtig 1976	Interplanetary Dust & Zodiacal Light	Proceedings of IAU Colloq. No. 31, many papers on solar system dust
Field & Cameron 1975	The Dusty Universe	Review articles on interstellar and solar system dust
Greenberg & van de Hulst 1973	Interstellar Dust & Related Topics	Proceedings of IAU Symp. No. 52, many papers covering nearly all aspects of interstellar dust
Huffman 1977	Interstellar Grains: The Interactions of Light with a Small Particle System	Extensive review of interstellar dust, includes a review of the bulk optical properties of solids of astronomical importance
McDonnell (1978)	Cosmic Dust	Review articles on interstellar and solar system dust
Merrill 1977	Infrared Observations of Late Type Stars	Review of infrared observations of circumstellar dust
Ney 1977	Star Dust	Review of circumstellar dust
Salpeter 1977	Formation and Destruction of Dust Grains	Review of theories of dust formation and destruction
Spitzer 1978	Physical Processes in the Interstellar Medium	Chapters 7, 8, and 9 of this graduate level text concern interstellar grains
Stein 1975	Recent Revelations of Infrared Astronomy	Review of the infrared emission from circumstellar dust
Wesson 1974	A Synthesis of Our Present Knowledge of Interstellar Dust	General review of interstellar dust
Wickramasinghe & Morgan 1976	Solid State Astrophysics	Collection of short papers on interstellar and circumstellar particles
Wickramasinghe & Nandy 1972	Recent Work on Interstellar Grains	Extensive review of interstellar dust
Wynn-Williams & Becklin 1974	Infrared Emission From HII Regions	Review of the infrared emission from heated dust

1977 and Merrill 1977). However, the relationship between circumstellar and interstellar grains is briefly discussed. While we concentrate on the observational side of this subject, we do not totally ignore theory since real progress is only made when observations and theory are interrelated.

The recent literature reviewing dust is extensive. Table 1 lists some of this literature, along with a brief description of aspects of cosmic dust covered by each reference. The book by Spitzer (1978) is a particularly useful introduction to the subject of interstellar dust. Aannestad & Purcell (1973), Huffman (1977), and Greenberg (1978) include more extensive discussions.

1   Interstellar Extinction

Extinction refers to the sum of absorption and scattering and is generally determined by comparing observations of reddened and unreddened stars assumed to have identical intrinsic energy distributions. Observed differences are attributed to extinction but may also reflect a breakdown
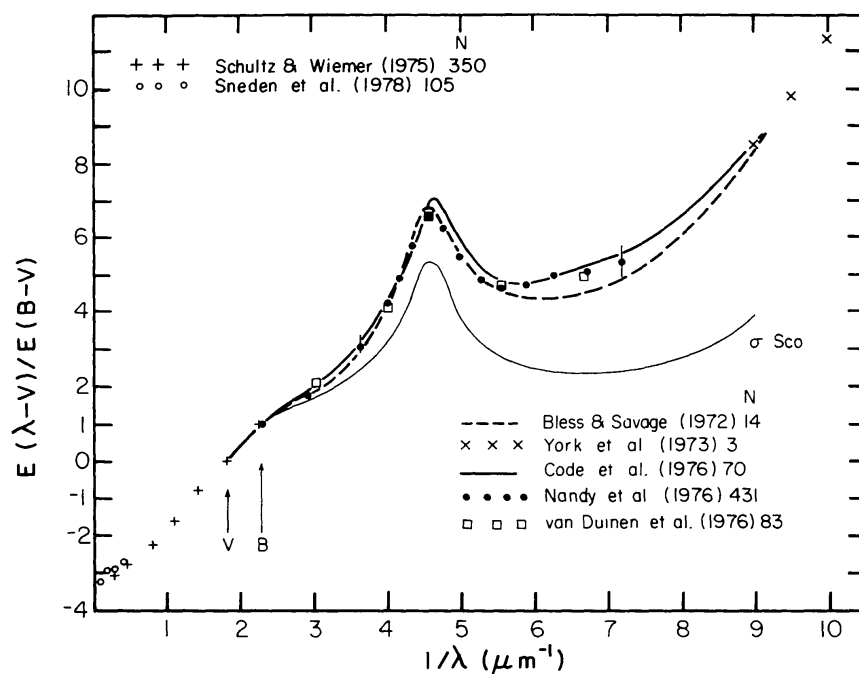

Figure 1   Average normalized interstellar extinction is plotted versus $1/\lambda$ in μm^{-1}. $E(\lambda-V)$ refers to the extinction in magnitudes between a wavelength λ and the photoelectric V band. The references for the various curves are provided along with an indication of how many stars were used to derive each average curve. One abnormal ultraviolet curve for σ Sco from Bless & Savage (1972) is also shown. The average curves plotted can be converted to total normalized extinction, $A_\lambda/E(B-V)$, by adding $R = 3.1$ to the quantity plotted. Note that the normalization to $E(B-V) = 1$ implies a corresponding hydrogen column density of $N(HI + H_2) = 5.8 \times 10^{21}$ atoms cm^{-2} (see Section 2). The error bars on two of the TD-1 points (Nandy et al. 1976) give an indication of the maximum observed variation in the *average* extinction curves derived for different galactic regions.

of the basic assumption above. Since the review of Aannestad & Purcell (1973) a considerable effort has gone into investigations of the wavelength dependence of extinction. While most observers appear to agree on the general characteristics of the extinction curve, the question of variations in the shape of the curve in localized galactic regions is still controversial, particularly in the IR. Average normalized extinction curves from a number of recent determinations are collected together in Figure 1. Here $E(\lambda-V)/E(B-V)$ is plotted against λ^{-1} in μm^{-1}. $E(\lambda-V)$ refers to the extinction in magnitudes between a wavelength, λ, and the V band of the photoelectric UBV system. $E(B-V)$ is the $(B-V)$ color excess in magnitudes. The relation between the quantity plotted and the total extinction, A_λ, at a wavelength λ is

$$A_\lambda/E(B-V) = E(\lambda-V)/E(B-V) + R,$$

where $R = A_V/E(B-V) \approx 3.1$ but is somewhat variable (see Sections 1.1 and 4.1).

In the following sections we discuss IR and visual extinction (Section 1.1) and UV extinction (Section 1.2). Within each section we consider the broadband aspects of extinction, fine structure in the extinction, and variation in the curve shape from region to region or from object to object. The extinction fine structure in the visual, commonly referred to as the diffuse interstellar features, is considered separately in Section 7. An average extinction curve representing a combination of IR, visual, and UV measurements is given in Section 1.3.

1.1   INFRARED AND VISUAL EXTINCTION   Extinction measurements in the IR are potentially subject to large systematic errors, since it is difficult to ensure that the reddened star and comparison star are intrinsically identical. The major problem is that some stars exhibit IR emission from heated circumstellar dust or free-free gaseous emission processes. A related but less severe problem can occur in the vicinity of 3600 Å if there are differences in the strength of the Balmer discontinuity between the reddened star and comparison star. A way around these problems is to exclude from the observing lists any object suspected of having a circumstellar envelope that might produce excess IR emission. Unfortunately, when such objects are excluded, the opportunities for studying the abnormal extinction characteristics of disturbed dust situated near hot or cool luminous stars are often eliminated. Also, it is not always easy to identify stars with excess IR emission and the criteria for identification often differ from one observer to another.

Several recent papers, which pay attention to these problems, present extinction measurements extending into the IR. Schultz & Wiemer (1975)

analyze a large collection of published observations of O and B stars obtained in the standard BVRIJKL filter bands but reject peculiar objects such as Be stars, stars with abnormal spectra, and close visual binaries. From color-color plots for a group of 350 stars they derive the mean extinction values illustrated with the plus symbols in Figure 1. Approximately 90% of the objects investigated follow the illustrated extinction relation. The remaining 10% of the objects deviate significantly either because of the presence of a circumstellar IR excess or because of real differences in the character of their extinction curves. Schultz & Wiemer prefer the former explanation. In a similar investigation, Sneden et al. (1978) obtain IR measurements of 105 stars near 2.3, 3.6, 4.9, 8.7, 10, and 11.4 μm. By eliminating stars with known emission characteristics, these authors derive the mean extinction results shown with the open circles in Figure 1. The data for the three long wavelength bands were combined and plotted at $\lambda^{-1} = 0.1$ μm^{-1}. In the region of overlap, the Schultz & Wiemer (1975) and Sneden et al. (1978) results agree reasonably well and appear to define a reliable average extinction curve (see Section 1.3). In estimating an average value of $R = A_V/E(B-V)$ from the data illustrated in Figure 1, Schultz & Wiemer obtain $R = 3.14 \pm 0.10$ while Sneden et al. obtain $R = 3.08 \pm 0.15$. These values of R are in reasonable agreement with other recent determinations by the color difference method and by other methods (see Sneden et al. 1978 and Schalén 1975 for additional discussion and comparisons). The error estimates for the derived values of R are somewhat misleading since assumptions must be made about the extrapolation of extinction from the longest wavelength IR measurements to infinite wavelengths. Changes in the character of this extrapolation can appreciably influence the estimate of R. For instance, the difference between A_λ varying as λ^{-1} versus λ^{-4} for $\lambda > 2$ μm introduces a difference of ~ 0.2 in the derived value of R (Sneden et al. 1978). For the remainder of this paper we adopt the value $R = 3.1$ as being consistent with the highest quality modern determinations.

In addition to the broadband aspects of the visual and IR extinction discussed above, there exists fine structure. In the visual there are the diffuse interstellar features with half-intensity widths ranging from 1 to 20 Å (see Section 7) and the very broad structure sometimes referred to as the VBS. In the IR, absorption features are found at 3.07 μm and 9.7 μm.

Hayes et al. (1973) discuss the existence of very broad structure with widths of 500 to 1000 Å superimposed on the visible extinction curve. The structure is of low amplitude and therefore difficult to measure. However, a number of independent investigations reveal roughly similar results (Whiteoak 1966, Hayes et al. 1973, Schild 1977) and the reality of

3S

3S

3S

the structure appears established. In the published curves the most convincing feature is a broad depression in the extinction curve between $\lambda^{-1} \approx 1.5$ and 2 μm^{-1}. For $E(B-V) = 1.0$, the amplitude of the depression is ~ 0.1 mag. Huffman (1977) notes the resemblance between the VBS and the absorption produced by terrestrial and meteoric magnetite (Fe_3O_4).

An absorption feature at 9.7 μm is found in many objects embedded within molecular clouds (Merrill, Russell & Soifer 1976). This feature also occurs in emission in stars and nebulae (Merrill & Stein 1976a,b) in which the dust is circumstellar or otherwise heated, and is almost certainly produced by silicates (see Section 8). Absorption at 9.7 μm has been detected in only two objects in which most of the intervening dust is in the ordinary interstellar medium (diffuse clouds as opposed to molecular clouds): the Galactic center and the star VI Cyg No. 12 (= Cyg OB2 No. 12). However, the dust obscuring these objects does not necessarily have a particularly large concentration of the carrier of the feature; one would not expect the feature to be observable in ordinary stellar spectra, because several magnitudes of extinction at V are required before the optical depth at 9.7 μm becomes appreciable. For the ordinary interstellar medium, this much extinction requires a large distance unless there is an atypically large concentration of dust along the line of sight. In general, the heavy extinction and great distance preclude detecting the features in even the brightest individual stars. However, the concentration of stars at the Galactic center (Oort 1977, Neugebauer et al. 1978) provides a suitably bright source, and the path length includes about 30 mag visual absorption (Becklin et al. 1978), almost all of which is in diffuse clouds not connected with the center itself. Similarly, the B8 Ia star VI Cyg No. 12 has $E(B-V) = 3.25$, or $A_V \approx 10$ mag, and no sign of an infrared excess (Johnson 1968). It is one of the intrinsically brightest stars in the Galaxy, with $M_V \approx -10$ (which is 3 mag brighter than a normal B8 Ia), and happens to lie behind a great concentration of apparently normal dust.

The 9.7 μm absorption feature has also been detected in several IR sources that lie behind very dense cold molecular clouds associated with normal or compact H II regions (Gillett et al. 1975a, Willner 1976, 1977, Persson, Frogel & Aaronson 1976). The feature is found in great strength in the spectrum of the Becklin-Neugebauer (BN) object in the Orion molecular cloud (Gillett & Forrest 1973). However, it is not possible to determine the optical depth of the feature very accurately by comparing the observed profile with that of the source, because the source's intrinsic emission profile is not known. One would expect the feature to be in emission when the dust is heated by luminous stars, as it is in the

Trapezium (Forrest, Gillett & Stein 1975). It is remarkable that the profiles of the 9.7 μm feature are very similar, in a wide variety of objects, over a considerable range of optical depths. The feature is broad ($\Delta\lambda/\lambda \sim$ 0.5) and has an asymmetric wing extending out to about 13 μm. It is broader than the feature in any naturally occurring terrestrial or lunar rock. However, its width agrees very well with laboratory measurements of disordered silicates produced by bombardment with energetic particles (Krätschmer & Huffman 1979) or produced in smoke (Day 1976).

Another IR absorption feature is found near 3.07 μm. It is commonly ascribed to solid H_2O and NH_3. In contrast to the 9.7 μm feature, it is (a) never found in emission, and (b) not found outside of molecular clouds, among which it has a highly variable strength relative to the 9.7 μm feature. Gillett et al. (1975b) have discussed the absence of absorption at 3.07 μm in the spectrum of VI Cyg No. 12. They find $\tau(3.07 \ \mu\text{m}) \leq 0.02$, so $A_V/\tau(3.07 \ \mu\text{m}) \geq 500$. Similarly, after a careful search, Soifer, Russell & Merrill (1976) failed to observe 3.07 μm absorption in the spectrum of the Galactic center, and find $A_V/\tau(3.07 \ \mu\text{m}) \geq 110$. On the other hand, the feature is strong in BN (Becklin & Neugebauer 1967, Gillett et al. 1975b) and in several other sources in molecular clouds (Merrill, Russell & Soifer 1976). The ratio $\tau(3.07 \ \mu\text{m})/\tau(9.7 \ \mu\text{m})$ differs widely among these molecular clouds, from 0.2 to 2, too large a variation to be explained by errors in the estimates of the optical depths. Gillett et al. (1975b) find that $\tau(3.07 \ \mu\text{m})/\tau(9.7 \ \mu\text{m}) < 0.04$ for VI Cyg No. 12, clearly quite different than for molecular clouds. NGC 2024 No. 1 and No. 2 (Merrill, Russell & Soifer 1976) convincingly show the association of the 3.07 μm feature with the inner regions of molecular clouds, and not with the outer regions or with the ordinary interstellar medium. No. 1, an early type star with $A_V \approx 8.3$ mag, lies in front of the core of the NGC 2024 molecular cloud, and has $\tau(3.07 \ \mu\text{m}) \leq 0.05$, so $A_V/\tau(3.07 \ \mu\text{m}) > 165$. No. 2, physically nearby No. 1 but behind the core of the cloud, has $A_V \sim 40 \pm 10$ mag (Hudson & Soifer 1976) and $A_V/\tau(3.07 \ \mu\text{m}) < 45$. The interstellar component is presumably similar in the two stars.

The relative width ($\Delta\lambda/\lambda$) of the 3.07 μm feature is a factor of three narrower than that of the 9.7 μm feature and is asymmetric towards longer wavelengths. It is easily distinguished from the narrow, symmetrical feature seen in the spectra of cool carbon stars (Merrill & Stein 1976a ; see their Figure 4). Hoyle & Wickramasinghe (1977) have suggested that the 3.07 and 9.7 μm features are both produced by interstellar polysaccharides. However, the very large variation in the relative strength of these two features speaks against this speculation (Egan & Hilgeman 1978).

The 18–22 μm flux distribution for several H II regions exhibits an

emission or absorption feature with deviations from the nearby continuum of about 30% (Forrest & Soifer 1976, Forrest, Houck & Reed 1976, Frogel, Persson & Aaronson 1977). Silicates show such a feature and this is taken to confirm the identification of the 9.7 μm feature with silicates.

The question of differences in the shape of the IR and visual extinction curve from region to region or object to object is controversial because of the observational complications outlined in the first paragraph of this section. Often highly contradictory conclusions are obtained because at the outset one kind of study eliminates objects surrounded by disturbed dust while another includes such objects. Different conclusions are sometimes obtained because different stars and regions are sampled. For example, Johnson (1977) still contends that the extinction curve for the Orion Trapezium region is abnormal while Penston, Hunter & O'Neill (1975) claim a normal reddening law in the Orion nebula cluster. Penston, Hunter & O'Neill base their conclusions on stars more than ~ 1.5 min from the Trapezium. However, scattered light measurements near θ^1 Orionis imply a gas-to-dust ratio that varies with position, so the dust near the Trapezium must have been modified (Schiffer & Mathis 1974). The Orion Trapezium extinction curve derived by Johnson (1977) exhibits large deviations from the normal curve for $\lambda < 1$ μm and significant contamination from free-free emission and/or heated dust seems unlikely at these wavelengths. In addition, Johnson notes that the hydrogen Paschen lines for θ^1C Ori and θ^1D Ori are of normal strength, which would appear to preclude a substantial amount of filling in by continuous IR emission. While it is possible to dispute the far IR portion ($\lambda > 2$ μm) of the Orion Trapezium extinction curve because of potential nebular and circumstellar contamination (Ney, Strecker & Gehrz 1973), it appears established that the Orion Trapezium extinction is abnormal for $\lambda < 1$ μm.

ρ Oph and HD 147889 are two other objects for which the case for abnormal IR and visual extinction seems reasonably secure (Whittet, van Breda & Glass 1976, Whittet & van Breda 1975). Both stars are situated in the complex of clouds that includes the ρ Ophiuchus dark cloud. The data suggest values of R significantly larger than 3.1. McMillan (1978) shows for HD 147889 that the 3.07 μm ice feature is absent [$\tau(3.07) < 0.01$]. Therefore, the large value of R for this particular line of sight is not produced by ice mantles.

Small differences in the visual and IR extinction from region to region appear in the average curves Johnson (1977) presents for Scorpius, Cygnus, Ophiuchus, and Perseus. Unfortunately, it is difficult to evaluate from the published results the extent to which stars with potential IR emission problems were rejected. However, the reasonably good cor-

relations between IR extinction curve shape indicators and the wavelength of maximum linear polarization (see Section 4) provide strong support for the reality of both small and large variations in the shape of the visual and IR extinction curve.

1.2 ULTRAVIOLET EXTINCTION   A number of satellites have provided extensive UV extinction measurements. These include: OAO-2 (Bless & Savage 1972, Savage 1975, Code et al. 1976), *Copernicus* (York et al. 1973), TD-1 (Nandy et al. 1975, 1976), and ANS (van Duinen, Wu & Kester 1976). In Figure 1, some of the average extinction curves from these satellites are plotted along with an abnormal curve for σ Sco. The different *average* UV extinction curves agree quite well. The small differences can probably be explained by bandpass effects and by true differences in the extinction between the different star samples used to obtain the averages. For example, the Bless & Savage (1972) average curve is probably lower in the region $\lambda^{-1} = 5$ to $8 \ \mu m^{-1}$, since the group of stars used to obtain the average contained a significant percentage from the Scorpius region, a region that exhibits low far UV extinction. The slight shift in the position of the extinction bump between the Code et al. (1976) curve and the rest of the curves may be the result of bandpass effects, since the Code et al. results are based on a combination of OAO-2 10 to 20 Å resolution scanner observations and broadband photometry observations of 70 stars.

The most remarkable aspect of the UV portion of the extinction curve is the broad bump centered near 4.6 μm^{-1} or 2175 Å. It appears that the feature is roughly symmetrical with a full width at half strength of about 1 μm^{-1} or 480 Å (Savage 1975). However, these estimates depend on the base line assumed. With a different choice, Nandy et al. (1975) obtain a full width at half strength of 360 Å. The position of peak absorption is remarkably constant although there may be some regions where the feature is shifted by about ± 50 Å from its normal position of 2175 Å (Savage 1975). The feature strength correlates well with $E(B-V)$ (Savage 1975, Nandy et al. 1976, Dorschner, Friedemann & Gürtler 1977). However, a few exceptions do exist. The most notable cases are θ^1 and NU Orionis, where the bump is weaker than normal (Bless & Savage 1972, Savage 1975, Savage & Bohlin 1978), and HD 156385 and HD 192163, where the bump is about one magnitude stronger than expected on the basis of estimates of $E(B-V)$ (Willis & Wilson 1975, 1977). The latter two objects are both Wolf-Rayet stars; HD 156385 is classified WC7, while HD 192163 is classified WN6. Circumstellar 2175 Å absorption also appears to exist in the spectrum of HD 45677 (Savage et al. 1978), a peculiar Be star with an enormous infrared excess due to circumstellar

dust. It is noteworthy that the IR excess for this object resembles the emission from the dust shells surrounding carbon stars and WC9 stars. The 2175 Å feature has also been detected in the Large Magellanic Cloud (Koornneef 1978a) and possibly in a number of additional external galaxies and in quasars (Baldwin 1977, Wu 1977a,b). The feature is, thus, of universal significance, and possible explanations for its existence are given in Section 8. At present, small graphite particles must be considered the most plausible cause.

At shorter UV wavelengths the extinction curve exhibits a minimum followed by a rapid extinction rise. A broad weak local enhancement in extinction appears in the TD-1 extinction curves near 6.3 μm^{-1}, but the reality of this feature is not established (Koornneef 1978b), though we note that it is quite pronounced in the TD-1 average curves for the Orion-Monoceros region given in Nandy et al. (1976). Attempts to find diffuse features between 3600 and 1100 Å are discussed in Section 7.

In the far UV, variations in extinction from object to object can be large. An extreme case, that of σ Sco, is illustrated in Figure 1. The curve shown is an OAO-2 measurement from Bless & Savage (1972). This result has been confirmed with the spectrometer aboard the *Copernicus* satellite (Snow & York 1975). This confirmation, with a telescope having an entrance aperture so small that nebular contamination is unlikely, is significant since there was concern with the OAO-2 measurements that nebular contamination may have produced some of the abnormal UV results.

Recently, the International Ultraviolet Explorer (IUE) satellite was used to obtain extinction curves toward $\theta^1 C$ and $\theta^1 D$ Orionis (Savage & Bohlin 1978) and these new results confirm the general character of the OAO-2 curve of Bless & Savage (1972) for θ Ori (both θ^1 and θ^2) that also exhibits an abnormally low far-UV extinction. Thus, there is little doubt that large far-UV extinction variations occur for some localized galactic regions. The most convincing cases are for regions of reflection and/or emission nebulosity where the dust is situated close to hot luminous stars. Observed variations in the extinction curves, particularly for highly disturbed regions, provide significant clues about the origin of the UV extinction. In order to explain the observed shape differences it may be necessary to invoke multicomponent grain models (Bless & Savage 1972).

Investigations of the more subtle regional variations in UV extinction by different observers have lead to contradictory results. Nandy et al. (1976) divided TD-1 UV extinction observations of several hundred stars into nine groups according to their galactic positions, derived mean extinction curves for each group, and claimed that none of the curves

deviated significantly from the grand average TD-1 curve illustrated in Figure 1. The maximum deviations found by Nandy et al. (1976) for these *mean* regional extinction curves, which they ascribe to errors, are illustrated with the vertical bars on some of the TD-1 data points in Figure 1. However, Koornneef (1978b) has re-analyzed the TD-1 data and concludes that definite regional extinction variations do exist.

Diffuse nebulae possibly provide information regarding the absorption properties of dust in the very far UV H- and He-ionizing portion of the spectrum (Mezger, Smith & Churchwell 1974, Panagia & Smith 1978). This suggestion is, however, quite controversial (see Brown, Lockman & Knapp 1978). Fairly elementary considerations (basically, simple photon counting) show that the He^+ and H^+ zones surrounding a hot star should be coincident if the central star is hotter than about 33,000 K (08 V). However, in Sgr B2 (Thum et al. 1978, Chaisson, Lichten & Rodriguez 1978) and in Orion (Peimbert & Torres-Peimbert 1977) the He^+/H^+ ratio is observed to be smaller than the cosmic abundance ratio (~ 0.1), indicating the ionized zones are not the same size. A reasonable explanation is that the absorption (not extinction) cross-section of the dust is about twice as large for helium-ionizing photons ($h\nu > 24.6$ eV) as for hydrogen-ionizing (12.6 eV $< h\nu < 24.6$ eV), so that the He^+ zone is reduced in size, relative to H^+, by dust absorbing its ionizing photons. Furthermore, nebular models (Balick 1975, Sarazin 1976) predict lower abundances for low stages of ionization (O^+, S^+, N^+, etc.) than are observed. The selective absorption by dust of radiation with $h\nu > 25$ eV over less energetic photons will explain this discrepancy as well. Finally, one can observe many giant H II regions in which there must be several O stars. There is a large spread in the He^+/H^+ ratios, as deduced from radio recombination lines (Panagia & Smith 1978). Emerson & Jennings (1978) show that those nebulae with the lowest He^+/H^+ ratio have the largest fraction of their ionizing photons absorbed by dust, although there are considerable observational uncertainties which make the correlation controversial. A serious objection to dust absorbing He-ionizing photons selectively is that no known substance has this property (Huffman 1977); in fact, the measured optical constants of graphite, silicates, etc., indicate that the absorption should peak at some 15 eV and then decline beyond the helium ionization edge.

1.3   AN AVERAGE EXTINCTION CURVE   Table 2 provides an average extinction curve extending from $\lambda^{-1} = 0$ to 10 μm^{-1}. This curve should be useful in correcting astronomical data for the effects of extinction. The curve represents a composite of the individual curves illustrated in Figure 1. However, an attempt was made to smoothly join the various

sections. For the various regions the following measurements were adopted: for $\lambda^{-1} = 0$ to 0.5, the results of Sneden et al. (1978) and Schultz & Wiemer (1975) were averaged and $R = A_V/E(B-V)$ was assumed to be 3.1 which is consistent with a simple extrapolation of these data; for $\lambda^{-1} = 0.5$ to 2.3 the Schultz & Wiemer (1975) results were used; for $\lambda^{-1} = 2.3$ to 7 we use the Nandy et al. (1976) TD-1 data; for $\lambda^{-1} = 7$ to 9 the Code et al. (1976) OAO-2 results are employed; and for $\lambda^{-1} = 9$ to 10 the York et al. (1973) measurements for ξ Per, ζ Per, and α Cam were averaged. Anyone using this curve should always bear in mind that regional differences may be present. Also, objects may exist for which this average curve is completely inappropriate. For example, in the case of σ Sco at $\lambda^{-1} = 8$ μm^{-1} an observed value of $E(\lambda-V)/E(B-V) = 2.8$ is more realistic. But such large deviations from the average curve seem rare.

Table 2   An average interstellar extinction curve

	$\lambda(\mu m)$	$\lambda^{-1}(\mu m^{-1})$	$E(\lambda-V)/E(B-V)$	$A_\lambda/E(B-V)$
	∞	0	-3.10	0.00
L	3.4	0.29	-2.94	0.16
K	2.2	0.45	-2.72	0.38
J	1.25	0.80	-2.23	0.87
I	0.90	1.11	-1.60	1.50
R	0.70	1.43	-0.78	2.32
V	0.55	1.82	0	3.10
B	0.44	2.27	1.00	4.10
	0.40	2.50	1.30	4.40
	0.344	2.91	1.80	4.90
	0.274	3.65	3.10	6.20
	0.250	4.00	4.19	7.29
	0.240	4.17	4.90	8.00
	0.230	4.35	5.77	8.87
	0.219	4.57	6.57	9.67
	0.210	4.76	6.23	9.33
	0.200	5.00	5.52	8.62
	0.190	5.26	4.90	8.00
	0.180	5.56	4.65	7.75
	0.170	5.88	4.77	7.87
	0.160	6.25	5.02	8.12
	0.149	6.71	5.05	8.15
	0.139	7.18	5.39	8.49
	0.125	8.00	6.55	9.65
	0.118	8.50	7.45	10.55
	0.111	9.00	8.45	11.55
	0.105	9.50	9.80	12.90
	0.100	10.00	11.30	14.40

2 *Distribution of Dust and the Dust-to-Gas Ratio*

Dust is primarily confined to the galactic plane with an effective thickness (two scale heights) of about 200 pc. The average reddening per unit distance determined for stars in the plane at 1 kpc is 0.61 mag kpc^{-1} (Spitzer 1978). For $R = A_V/E(B-V) = 3.1$ this implies an average total extinction at the visual band of 1.9 mag kpc^{-1}. However, the distribution of the obscuring dust is very patchy. There are directions where the reddening per unit distance deviates by large factors (5 to 10 times) above or below the average. The irregular distribution of absorbing matter is clearly delineated in the extinction maps of FitzGerald (1968) and in the extinction contour plots of Lucke (1978). Lucke has updated the work of FitzGerald by determining the color excesses and photometric distances for ~ 4000 O and B stars using data from a number of recent photometric and spectroscopic catalogues. These results were then used to construct a number of contour plots of extinction that provide a three-dimensional picture of the distribution of large dust complexes in the local region of the galaxy. Perpendicular to the plane, a cosecant distribution, which is often assumed for extragalactic studies, is a poor representation of the absorption. The paper of Heiles & Jenkins (1976) is particularly useful for visualizing the distribution of interstellar matter. In this work, photographic representations of the galactic distribution of HI are provided for $|b| \geqq 10°$. In addition, plots on a similar scale are given for interstellar linear polarization, the dark nebulae of Lynds (1962), the bright nebulae of Lynds (1965), and a photographic representation of the Shane & Wirtanen (1967) galaxy counts (which provides an estimate of the dust column density integrated to the edges of the galaxy). Only a few results have been reported so far on work in progress toward understanding the very local ($r < 200$ pc) distribution of dust (Strömgren 1972). For the very local material it is necessary to obtain precise estimates of $E(B-V)$ and to include A and F stars in the analysis in order to provide a reasonable sample of objects.

Extinction measurements are valuable in determining representative properties of interstellar clouds. Roughly speaking, the statistics of extinction imply the existance of ~ 6 "standard clouds" per kpc with $E(B-V)$/cloud of about 0.06, and ~ 0.8 "large clouds" per kpc with $E(B-V)$/cloud of about 0.29 (Spitzer 1978). Certainly the medium is more complex but the cloud concept provides a useful starting point for visualizing the patchy distribution of matter.

An improvement in our understanding of the association of interstellar dust and gas has been obtained through an extensive survey of interstellar atomic and molecular hydrogen with the *Copernicus* satellite (Savage et

al. 1977, Bohlin, Savage & Drake 1978). These measurements are superior to the OAO-2 measurements reported by Jenkins & Savage (1974) because the high resolution of *Copernicus* permits a clear separation of the interstellar absorption lines from troublesome stellar lines. Furthermore, only *Copernicus* has the far-UV wavelength coverage that is required to observe molecular hydrogen in absorption against hot stars. Atomic hydrogen, $N(HI)$, and the total hydrogen, $N(HI + H_2) = N(HI) + 2N(H_2)$, column densities are correlated with $E(B-V)$ in Figures 2a and b. These figures were produced by plotting linearly the data for 100 stars in Table 1 of Bohlin, Savage & Drake (1978). Be stars are denoted with the open symbols. The point for ρ Oph, which has an upward arrow attached, should be moved well off the figures to $N(HI) = 65 \times 10^{20}$ atoms cm^{-2} and $N(HI + H_2) = 72 \times 10^{20}$ atoms cm^{-2}. The correlation between dust and total hydrogen is significantly better than the correlation with atomic hydrogen. From the data shown in Figure 2b, Bohlin, Savage & Drake (1978) derive a weighted average total gas-to-color-excess ratio of
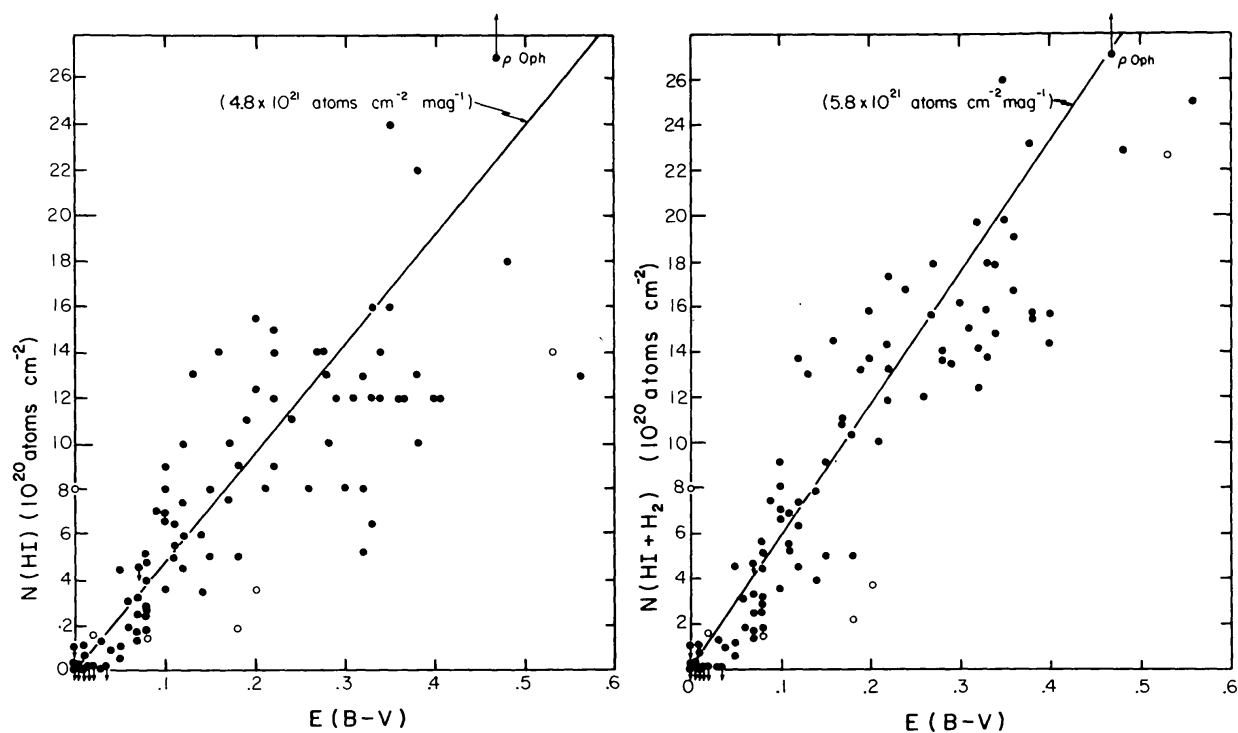
Figure 2   Correlations between gas column densities and interstellar reddening for 100 stars from the *Copernicus* atomic and molecular hydrogen survey (Savage et al. 1977, Bohlin, Savage & Drake 1978): (a) shows the atomic hydrogen column density, $N(HI)$, versus $E(B-V)$, (b) shows the total hydrogen column density, $N(HI + H_2) = N(HI) + 2N(H_2)$, versus $E(B-V)$. Be stars are denoted with the open symbols. The solid line in (a) gives the average *atomic* hydrogen to $E(B-V)$ ratio 4.8×10^{21} atoms cm^{-2} mag^{-1}. In (b) the solid line gives the average *total* hydrogen to $E(B-V)$ ratio of 5.8×10^{21} atoms cm^{-2} mag^{-1}. The point for ρ Oph in (a) and (b) should be moved upward by about a factor of 2.7.

$\langle N(HI+H_2)/E(B-V)\rangle = \Sigma N(HI+H_2)/\Sigma E(B-V) = 5.8 \times 10^{21}$ atoms cm^{-2} mag^{-1}. This average result is illustrated with the solid line. A correction for ionization in the H II regions surrounding the early-type stars used as sources will tend to increase this number somewhat. Jenkins (1976) has estimated that the correction might amount to about 4%. A comparison of Figures 2a and b shows that the effect of molecule formation on the estimate of the total gas column density begins to become important for $E(B-V) \gtrsim 0.1$. Recent estimates of the *atomic* hydrogen-to-color-excess ratio using 21-cm data are $\langle N(HI)/E(B-V)\rangle = 5.0 \times 10^{21}$ atoms cm^{-2} mag^{-1} by Burstein & Heiles (1978) and 5.1×10^{21} atoms cm^{-2} mag^{-1} by Knapp & Kerr (1974). These values are very similar to the value obtained from the *Copernicus* results in Figure 2a for HI alone of 4.8×10^{21} cm^{-2} mag^{-1} (Bohlin, Savage & Drake 1978). Perhaps ionization could explain the small difference. For stars with accurate $E(B-V)$ the scatter in Figure 2b about the average relation is generally less than a factor of 1.5. An important exception is the dark cloud star ρ Oph with $N(HI+H_2)/E(B-V) = 15.4 \times 10^{21}$ atoms cm^{-2} mag^{-1}. A reduction in the visual reddening efficiency for the larger than normal size grains in the ρ Oph region (Carrasco, Strom & Strom 1973, Whittet & van Breda 1975) possibly explains this result. A search should be made for other objects that might exhibit an anomalous gas-to-color-excess ratio as these observations may provide useful information about the growth of grains in dense regions. The gas-to-color-excess ratio is well established, at least for the local region of the Galaxy. However, the value, 5.8×10^{21} atoms cm^{-2} mag^{-1}, should be used with caution for dense clouds. The point for ρ Oph suggests that this ratio might increase significantly for dust in dense clouds.

A total gas-to-color-excess ratio of 5.8×10^{21} atoms cm^{-2} mag^{-1} combined with current grain theories such as the theory of Mathis, Rumpl & Nordsieck (1977) implies that approximately 0.7% by mass of the interstellar material in diffuse clouds is in the form of dust. However, this number should be considered a lower limit since very large grains could contribute significantly to the grain mass but not to the extinction.

3 Light Scattering by Grains

In this section, we consider direct observations of the scattered light from dust grains in both reflection nebulae and in the diffuse galactic light. The procedure is simple: one knows (or assumes) the geometry of the light sources and of the scattering dust. The geometry is idealized into a simple form (plane-parallel uniform slabs, spheres, etc.) for which radiative transfer calculations are practical. One assumes the properties (albedo and phase function) for individual scattering from single grains, calculates

the expected surface brightness from the dust distribution, and, finally, compares it to observations to determine the actual properties.

It has become traditional to calculate with the Henyey-Greenstein (1941) phase function, which is merely a convenient analytic function with two parameters, a, the albedo, and g, the average value of the cosine of the angle of scattering. Isotropic (or Rayleigh) scattering corresponds to $g = 0$, complete forward scattering to $g = 1$. The values of a and g are assumed to be arbitrary parameters to be varied until the predicted surface brightness matches the observed. Mie theory, for scattering from a sphere with a given size and index of refraction, provides analytic expressions for a and g. However, more than two parameters are required to characterize phase functions accurately. Therefore, the actual phase function of the sphere (also calculable from Mie theory) differs from the Henyey-Greenstein function of the same a and g. Besides showing complicated diffraction spikes, which are not important because integration over any reasonably broad size distribution washes them out, the actual pattern often shows a rather strong backscattering lobe not present in the Henyey-Greenstein function. This backscattering may be an artifact of the assumed spherical shape. On one hand, Zerull (1976) has experimentally measured the phase function for irregular particles. He finds fairly good agreement with Mie theory for $\theta = 180°$, but stronger scattering at intermediate angles. On the other hand, Chylek, Grams & Pinnick (1976) have also measured irregular particles and found the backscattering lobe to be virtually missing. At present, the situation is not clear. If the lobe is present, the phase function can be represented as the sum of two Henyey-Greenstein functions, one with $g < 0$ (Kattawar 1975).

We first consider the diffuse galactic light and the reflection by dark clouds, both of which are illuminated by the general stellar radiation field of the Galaxy. Next, we discuss reflection nebulae. We do not consider light scattered by dust inside H II regions (Isobe 1977). Such dust is known to be peculiar, as compared to the general interstellar medium, at least in the Orion nebula and M8.

3.1   THE DIFFUSE GALACTIC LIGHT   There have been many ground-based studies of the diffuse galactic light (DGL) (see Lillie & Witt 1976), all of which use a single Henyey-Greenstein function. Galactic models of varying complexity predict that interstellar dust is fairly efficient in scattering ($a \geq 0.4$, probably 0.7 ± 0.1). The values of a and g are not determined independently; a large value of g (~ 1) corresponds to a low value of a, and vice versa. The value of g is not well determined ($g = 0.7 \pm 0.2$), but must be large to avoid values of the albedo close to or

exceeding unity. The data are not accurate enough to distinguish differences in a and g in the U, B, or V bandpasses. The physical reason why a low a must accompany a high g is that one sees readily detectable amounts of DGL only near the plane of the Galaxy, where there is a large amount of direct starlight as well. If g is large, most scattered photons have been deviated only slightly, and the scattered intensity is determined by the bright stellar background behind the dust. Conversely, with a lower g (i.e. a more isotropic phase function), the dust scattering depends more on the average value of the sky brightness, which is much lower than the value in the Galactic plane. Consequently, one needs a higher albedo to provide the same (observed) value of the DGL.

A basic problem in the visible spectral region is the faintness of the DGL in comparison to other sources of sky brightness. Averaged over the entire sky, at 5300 Å the zodiacal light, direct starlight, and DGL have brightness of 200, 100, and 35 S_{10}'s (Roach & Megill 1961), where one S_{10} is the surface brightness corresponding to one tenth-magnitude AO V star per square degree. In general, the brightness of the stars is uncertain by at least 20%. The uncertainty in the magnitude of the zodiacal light is large in comparison to the probable value of the DGL near the Galactic pole. At the Galactic equator, the the brightness of the DGL is not badly determined; about 70 S_{10} in Cygnus (along a spiral arm) at 5300 Å, and some 170 S_{10} for stars (Witt 1968). The contribution of stars within a single small area of the sky in which observations are made can be assessed by careful photometry. However, the illumination of the dust seen in that small area is from the irregularly fluctuating distribution of stars along the entire line of sight. The incident illumination is especially uncertain for dust clouds at some distance above the plane of the Galaxy, where the radiation field is expected to be quite different from the local one. Furthermore, the various dust clouds have a lower effective a and g than the individual particles in them (Mattila 1971).

In the UV spectral regions, observations are available from OAO-2, with a number of channels in the range $4250 \geqq \lambda \geqq 1550$ Å. With the assumption that $g = 0.7$, Lillie & Witt find that $a = 0.6$ for $\lambda = 1550$ Å, $a = 0.4 \pm 0.1$ for $1800 \leqq \lambda \leqq 2200$, and a increases to 0.7 ± 0.1 at $\lambda \geqq 3300$. Morgan, Nandy & Thompson (1976), using another model for the radiation field, find consistent results; $a(2350$ Å$) \approx 0.7a(2740$ Å$)$, if g is constant over that range. However, there is appreciable additional uncertainty in a (perhaps several tenths) arising from the possibility of g's changing with wavelength.

The data do not require a dramatic change in either a or g across the 2200 Å bump; a seems to decline smoothly across the bump as λ decreases.

Hence, both the absorption and scattering cross-sections apparently reach a maximum there, and the bump cannot be ascribed unambiguously to either process.

The problems with UV studies of the DGL are rather different from the visual. On one hand, since the sun is comparatively faint in the UV, one has far less zodiacal light to contend with. On the other, the stellar illumination field was not known when the studies were made, and there are significant discrepancies among various observations and predictions for that field. For instance, the total radiation field at 1530 Å (DGL and stars) has been observed by Henry et al. (1977) for the northern hemisphere sky. They find very good agreement with Lillie & Witt at the Galactic equator, but obtain a mean brightness of about 60 S_{10} averaged over the sky. Lillie and Witt based their DGL analysis on a model of the stellar radiation field of Witt & Johnson (1973), which predicted a mean brightness of about 90 S_{10}. This difference indicates the difficulty of predicting the high-latitude stellar radiation field upon which the value of the DGL depends. Furthermore, the illumination is described far less well by the plane-parallel slab models for the star and dust. In fact, most of the local radiation at 1500 Å comes from rather bright stars, $m_V \lesssim 4$ (Henry 1977), which have an irregular distribution along the Gould belt. The clumping of the dust into clouds is also a much more severe problem in the UV than in the optical range.

3.2   SCATTERING FROM DUST CLOUDS   Another means of determining the optical properties of dust is from the surface brightness of dark nebulae that are reflecting radiation from the Galaxy. Mattila (1970) determined the absolute surface brightnesses of a low-latitude and of a high-latitude dark cloud. The predicted brightness of the cloud depends on the (a,g) values assumed for the grains in it, the optical depth of the cloud, and the density distribution assumed within the cloud. The values of a and g that explain the brightness of a cloud in Taurus ($b = 0°$) are similar to those from the DCL, with a increasing if g decreases. The interesting feature is that for clouds at high latitude, acceptable values of a and g increase *together*, for reasons discussed by Mattila (1970). Hence, if one assumes that dust in both high- and low-latitude clouds is intrinsically the same, the acceptable solutions cross at a steep angle in the (a,g) plane, and a and g are well determined. For 4300 Å, Mattila obtains $a = 0.65$, $g = 0.85$, similar to the DGL values. There are, however, difficulties with the method; the results are sensitive to the density distribution assumed within the cloud, which Mattila took to be uniform. Furthermore, the strong backscattering lobe of the actual dust phase

function, not represented in a single Henyey-Greenstein function, possibly makes an appreciable difference.

FitzGerald, Stephens & Witt (1976) have used a different method to analyze scattering from dust clouds. They determine the brightness profile across the face of the "Thumbprint Nebula" relative to the adjacent sky brightness, so the photometry is differential. They compare the observations with predictions of a model with an r^{-2} density distribution. The nebula is 140 pc from the Galactic plane, so they rely upon a plane-parallel model of the Galaxy to provide the incident radiation field. They find that g is well determined for visible wavelengths at $g = 0.7$. The r^{-2} density distribution is suggested by star counts of the outer regions, but must be assumed within the regions for which it can not be verified. More seriously, the central optical absorption is large (17 mag at B), and the extinction appears to have $A_V/E(B-V) = 5.7 \pm 1.1$ instead of the normal value of 3.1. This large value is apparently characteristic of thick, dense clouds. Hence, one cannot confidently assume that the derived value of g applies to the normal interstellar medium.

Two reflection nebulae have recently received attention, the Merope Nebulosity in the Pleiades (Andriesse, Piersma & Witt 1977, Witt 1977) and the Orion Reflection Nebulosity (Carruthers & Opal 1977, Witt & Lillie 1978), which is the large, diffuse reflection extending over the entire constellation of Orion, containing Barnard's Loop and illuminated by the entire Orion cluster of OB stars. Unfortunately, in neither nebula is the geometry of the stars and dust very clear (Jura 1977). The wavelength variation of the scattered light, relative to the star(s), is consistent with a large contribution from an optically thick slab of dust behind the star(s), so that there is a large contribution from backscattered radiation. While no quantitative models have been fitted to the data, Andriesse, Piersma & Witt (1977), Witt (1977), and Witt & Lillie (1978) believe that the data indicate that one needs an almost isotropic ($g \leq 0.25$) phase function at 1550 Å, in marked contrast to Lillie & Witt's (1976) result of $g = 0.6$ for the DGL. This is a very important result, if true. If g is substantially lower than 0.7 at 1550 Å, which the DGL analysis of Lillie & Witt (1976) assumed, then the albedo must be appreciably increased for the reason stated at the beginning of Section 3.1. Furthermore, Lillie and Witt used a theoretical model of the radiation field that is now known to be too large, so the albedo must be increased further to compensate for the lower illumination that is actually present. Hence 0.6, the albedo claimed by Witt and Lillie at 1550 Å, is a strong lower limit to what would be necessary if g were ≤ 0.25. However, for classical scattering, i.e. in the absence of quantum mechanical effects, there is no distribution of particle

sizes that can simultaneously provide both low g and high a in the UV, since low g is only obtained in the Rayleigh limit (size $\ll \lambda/2\pi$) where the albedo must be low. Thus, if $g \leqq 0.25$ at 1550 Å, the scattering must be from some process other than classical scattering, such as that suggested by Platt (1956). We feel that it is important to determine to what extent the geometrical uncertainties in the reflection nebulae affect the interpretation of the observations.

In summary, in the visual region of the spectrum interstellar particles have $a \sim 0.7$ and $g \sim 0.7$. The albedo drops for $\lambda < 3000$ Å to about $a \sim 0.3$–0.4, if g remains at about 0.7. There is no evidence for dramatic changes in a or g in the vicinity of the extinction bump at 2200 Å. The phase parameter is not well determined, and variations in it would affect the derived albedo substantially. The situation for 1550 Å is quite unclear. The subject of the analysis of scattered light is controversial at present.

4   Interstellar Polarization

In this section, we discuss broad-band linear polarization, the linear polarization of narrower spectral features, and conclude with circular polarization.

4.1   LINEAR POLARIZATION   The linear polarization of stars in the $UBVR$ system is discussed by Coyne, Gehrels & Serkowski (1974) and Serkowski, Mathewson & Ford (1975). After all Wolf-Rayet and emission-line stars of luminosity classes III–V are eliminated, 364 stars remain, distributed over the entire sky. The polarization for each star reaches a maximum value, P_{max}, at some wavelength, λ_{max}, and there is a large spread in both quantities among the stars. However, a remarkable fact emerges: for all stars, the ratio $P(\lambda)/P_{max}$ is adequately fitted by a function of λ/λ_{max}: $P(\lambda)/P_{max} = \exp\left[-1.15 \ln^2 (\lambda/\lambda_{max})\right]$. The existence of such a scaling law implies that the optical constants of the polarizing material do not change with wavelength in the visual and near IR (Martin 1974), an important result that militates against graphite as the carrier of polarization, but allows dielectrics (silicates, ices, SiC, etc.). However, in the K (2.2 μm) band, Dyck & Jones (1978) show that the polarization is significantly higher than the expression would predict.

Serkowski, Mathewson & Ford (1975) find a good correlation of λ_{max} with the color ratio $E(V–K)/E(B–V)$, which was further tightened by improved IR photometry (Whittet & van Breda 1978). Table 2 and Figure 1 show that the quantity R, or $A_V/E(B–V)$, can be estimated from this color ratio by a short extrapolation from the K band (0.45 μm^{-1}) to infinite wavelength, so there is also a tight correlation of

λ_{max} with R:

$$R = (5.8 \pm 0.4)\,\lambda_{max}(\mu m),$$

where the constant of proportionality has been changed slightly from Whittet and van Breda's to reflect the extinction law of Table 2. This relation is very convenient to use for investigations of interstellar extinction, since one can substitute optical measurements of polarization for IR photometry. One must be cautious if light from the object may have intrinsic polarization (e.g. a Be star).

The average value of λ_{max} over the entire sky is 0.545 μm. However, as shown in Figure 6 of Serkowski, Mathewson & Ford (1975), there are regions (Orion, Scorpius, and Ophiuchus) where λ_{max} is significantly larger than average (up to 0.80 μm) and others (e.g. Cassiopeia and Cygnus) where it is smaller (down to 0.41 μm in the Cyg OB2 association). The regions of large λ_{max} are the denser clouds, and the large λ_{max} implies a larger than average particle size. The nearby stars also show a larger λ_{max} than average, presumably a selection effect because they must lie behind clouds of higher than average density in order to show measurable polarization.

The values of P_{max} are poorly correlated with $E(B-V)$, except that $P_{max}(\%)/E(B-V) \leqq 9$. The upper limit of $P_{max}/E(B-V)$ presumably arises in the most favorable case of large and uniform alignment along the line of sight, and puts very severe constraints on grain alignment mechanisms.

The above discussion refers to polarization in the ordinary interstellar medium. In IR sources associated with molecular clouds, extremely strong near-IR ($\lambda > 1.6$ μm) polarization has been found, over 15% in some cases (Dyck & Beichman 1974, Dyck & Capps 1978). These objects, obscured so heavily by dust that their polarization in the optical is unknown, are in regions of recent star formation. There is a strong inverse correlation between physical size of the objects and the strength of polarization.

Linear polarization across spectral features such as the diffuse interstellar bands (see Section 7), the $\lambda 2200$ bump, and the 9.7 μm silicate feature should increase if the carrier for the feature is also the aligned particle providing the continuum polarization. Measurements at $\lambda 2200$ for two stars (Gehrels 1974) fit onto the standard law for P/P_{max}, indicating that the carrier of the $\lambda 2200$ feature is not aligned. Clearly, higher spectral resolution UV polarimetry would be very interesting. There are two objects in which strong polarization in the 9.7 μm silicate feature has been observed, the Galactic center (Capps & Knacke 1976 and Knacke & Capps 1977), where $P(9.7$ μm$) \approx 6\%$, and the BN source associated with

the Kleinmann-Low nebula in Orion, where $P(9.7 \mu m) \approx 15\%$ (Dyck & Beichman 1974). Each has a sharp increase in $P(\lambda)$ at the wavelength of the feature. This is a direct detection of the alignment of the silicate grains, and suggests that they are not responsible for the $\lambda 2200$ bump. However, it should be emphasized that the 9.7 μm and 2200 Å polarizations have been measured in quite different types of objects. In BN, the grains are known to be different, since the 3.07 μm ice absorption is seen. Possibly, the alignment mechanisms are different. It would be very interesting to detect the 2200 Å and 9.7 μm polarizations in the same object.

The polarization of the 9.7 μm feature also shows that the continuum polarization of the KL nebula and of BN is caused by absorption from aligned grains, rather than by emission. Aligned grains emit radiation with the direction of polarization along the direction in which the absorption is greatest. On the other hand, radiation suffering absorption by the same grains would be polarized along the direction in which the absorption is least, or perpendicular to the direction for emission. There is no doubt that the 9.7 μm feature is in absorption, and the direction of its polarization is the same as that of the continuum, strongly suggesting that the continuum polarization is from absorption by the grains. The polarization direction for several regions in the Kleinmann-Low nebula is the same, making it unlikely that the polarization arises from reflection by dust clouds.

Martin (1975) shows how the wavelength dependence of the polarization across the 9.7 μm feature can be used to obtain an upper limit to the band strength (the extinction cross-section at band center, per volume of grain). A low value is indicated, about two or three times lower in both BN and the Galactic center than in terrestrial or lunar rocks, and 15 times smaller than for pure minerals. This low strength is characteristic of disordered silicates (Day 1976, Krätschmer & Huffman 1979), and presumably explains why the emission feature is so broad near the Trapezium. A very high degree of grain alignment is required to explain the observations; just how much depends on the optical depth at 9.7 μm, which is not directly observable but must be inferred using assumptions regarding the geometry of the source and dust.

4.2   CIRCULAR POLARIZATION   Linearly polarized light, passing through aligned grains, can become circularly polarized because the grains introduce a phase shift in one direction relative to another. The birefringence, or amount of phase shift per volume of grain, can be calculated for grains of various shapes if the index of refraction $m(= n-ik)$ of their material is known. Martin (1972, 1974) has discussed the interpretation

of circular polarization data. The most interesting feature is that its wavelength dependence is qualitatively different for a dielectric (a material with a small value of k), than for a metal (with k comparable to n). For a dielectric, such as a silicate, the circular polarization changes sign at some wavelength, λ_c. Furthermore, if $k = 0$, then $\lambda_c = \lambda_{max}$ (the wavelength at which the linear polarization is a maximum). As k increases for a given n, λ_c becomes progressively larger than λ_{max}. For metals with a wavelength-independent index, the circular polarization need not change sign; if it does, $\lambda_c \ll \lambda_{max}$. Thus, the difference of λ_c and λ_{max} is a measure of the value of k. Unfortunately, the value of k corresponding to a given value of λ_c–λ_{max} depends sensitively on the value of n as well. Furthermore, if n and k are both changing with wavelength it is possible that $\lambda_c \approx \lambda_{max}$, even if k is not small. Magnetite is an example of such a substance (Shapiro 1975).

Martin & Angel (1976) observed λ_c for a variety of objects with both small and large values of λ_{max} and found $\lambda_c = \lambda_{max}$ in all cases. Graphite is definitely excluded as the carrier of polarization, and a very small value of k (as in a good dielectric such as a silicate) is indicated. Further analysis can yield information regarding the changes in grain alignment along the line of sight and provide information about the Galactic magnetic field (Martin & Campbell 1976).

5 Heavy Element Depletion

Studies of the depletion of interstellar elements from the gas phase provide an indirect but powerful method for studying the interstellar dust. The term depletion refers to the factor by which the gas phase column density of an element is below that expected on the basis of a measured total hydrogen column density and the assumption of cosmic abundances. Generally, solar abundances are used for the reference abundance since only the sun has a reliable set of abundances covering a wide range of elements. Any enrichment of the interstellar medium since the formation of the sun will introduce errors in these reference numbers. However, the solar abundance scale, with only a few exceptions, appears to be very similar to the abundances found in O and B stars and in gaseous nebulae (see Salpeter 1977 for a discussion and references). The missing gas is assumed to be in the solid phase since observed molecular column densities can only explain a very small part of the measured depletions. The study of depletion has been greatly expanded by the unique observing capabilities of the *Copernicus* ultraviolet telescope. Since Spitzer & Jenkins (1975) and Salpeter (1977) reviewed this subject recently, we will emphasize current developments.

The accuracy of column densities of interstellar species determined

from absorption line measurements depends critically on curve-of-growth effects. As a general rule, column densities for species with few very weak or very strong (damped) lines have errors up to a factor of two, while column densities for species producing lines on the flat part of the curve of growth can easily have errors amounting to factors of 10 or more (Nachman & Hobbs 1973). Therefore, in evaluating the significance of depletion results, one must carefully examine the positioning on the curve of growth of the line or lines used in the analysis. Often the errors quoted in depletion papers do not include estimates of the large systematic errors that would occur if the adopted curve of growth is inappropriate for the species being analyzed. An additional uncertainty of perhaps a factor of two is introduced when one adopts the solar reference abundance. Finally, the most extensive data have been obtained at a velocity resolution of 13 km s^{-1}. Therefore, the measurements are often an average over a number of unresolved cloud components.

5.1   DETAILED STUDIES OF A FEW CLOUDS   The most extensive studies of depletion of many elements in a limited number of clouds are for ζ Oph and ζ Pup (Morton 1975, 1978), for γ Ara (Morton & Hu 1975), and for ζ Per and o Per (Snow 1976, 1977). Figures 3a and b illustrate results for lines of sight with moderate [ζ Oph, $E(B-V) = 0.32$] and low [ζ Pup, $E(B-V) = 0.04$] reddening. Depletion is plotted versus condensation temperature, which is defined in the caption. For ζ Oph the highly refractory elements such as Fe, Ni, Ti, Ca, and Al exhibit large depletions (factors of 50 to 10^4). Na, K, Li, Mn, P, Si, and Mg exhibit moderate amounts of depletion (factors of 10 to 30), while a few elements (S and Zn) exhibit practically no depletion. For the very important C, N, and O group, the depletion appears to lie between 1 and 5. The oxygen depletion is of crucial importance for interstellar grain theories since oxygen is the most abundant element after H and He. For ζ Oph, estimates of the oxygen depletion have changed considerably over the past few years, as illustrated in Figure 3a. The 1975 results are from Morton (1975) and were based on two strong lines. Zeippen, Seaton & Morton (1977) review the ζ Oph oxygen depletion and on the basis of measurements of the weak intersystem line at 1355 Å derive a depletion ranging from about a factor of two to a factor of three. However, recently de Boer (1979) reanalyzed the Zeippen, Seaton & Morton (1977) data and concluded from curve-of-growth considerations and a profile fit that the oxygen toward ζ Oph is only depleted by about 25%. This revised depletion is consistent with the oxygen's only being tied up in mineral grains such as enstatite, olivine, and magnetite and does not require the presence of ice coatings, consistent with the absence of the 3.07 μm "ice" feature toward

stars behind diffuse clouds (see Section 1.1). For nitrogen, Lugger et al. (1978) present results for ten lines of sight including ζ Oph, based on the analysis of NI lines ranging in f value from 10^{-6} to 10^{-1}. Since weak lines are included in the analysis, the results should be relatively reliable (factor of two errors) and indicate an average nitrogen depletion of a factor of two. This result, if correct, would appear to require the presence of solid NH_3, which is inconsistent with the missing 3.07 μm feature, although ultraviolet and cosmic ray processing of ice coatings has often been advocated as an explanation of the missing "ice" feature in diffuse clouds (Greenberg 1976, and references therein). However, considering the errors associated with abundance measurements, the result is also consistent with no nitrogen depletion. Unfortunately, the important carbon abundance is still very uncertain since only strong lines of C II have thus far been detected.

The correlation for reddened stars between depletion and condensation temperature was first pointed out by Field (1974). This correlation
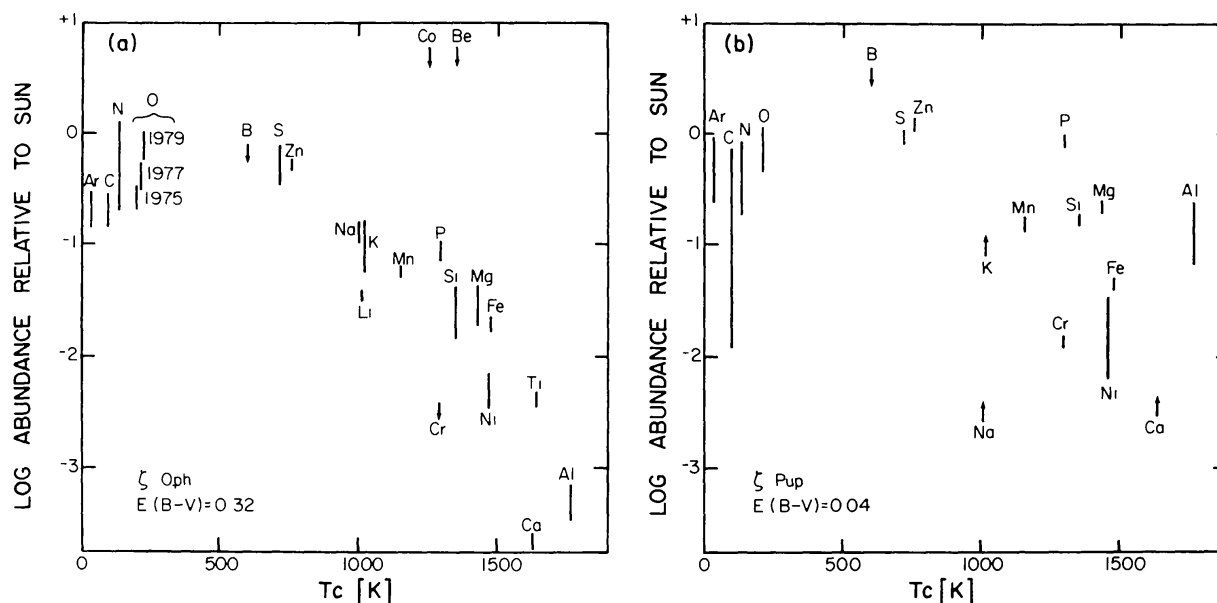
Figure 3 Elemental depletion is plotted versus condensation temperature for a moderately reddened line of sight in (*a*) and a lightly reddened line of sight in (*b*). The data are from Morton (1975) for ζ Oph in (*a*) and Morton (1978) for ζ Pup in (*b*). These results have been supplemented by more recent estimates of the oxygen abundance from Zeippen, Seaton & Morton (1977) and de Boer (1979). The nitrogen depletion plotted is from Lugger et al. (1978). The reference abundances are from Withbroe (1971) with the exception of the boron abundance which is from Boesgaard et al. (1974). Error bars are as given in the various publications. The condensation temperature is defined as the temperature at which half of a particular atom has condensed out of a gas of solar composition as it is slowly cooled but maintained in thermal and chemical equilibrium. If grains are formed in dense expanding circumstellar gas clouds under conditions of thermal and chemical equilibrium, then one might expect to see a correlation between depletion and condensation temperature (Field 1974).

possibly suggests that grain formation occurs under near equilibrium conditions in the dense environments in the vicinity of stars. However, Jura & York (1978) noted that recent equilibrium calculations suggest that P and Fe have similar condensation temperatures (1290 K versus 1335 K) but usually have very different depletions (2 to 3 for P and 30 to 100 for Fe). Also, Snow (1975) finds that with the exception of Li, Na, and K an equally good correlation exists between depletion and the first ionization potential of an element, which is perhaps related to the probability of an atom sticking to a grain's surface. Snow suggests that the non-correlation for Li, Na, and K is possibly related to the fact that these are the only elements that form chemically saturated molecules with hydrogen; Watson & Salpeter (1972) have argued that whenever such a molecule is formed on a grain it is immediately ejected. Thus, Snow's hypothesis is that the depletion pattern is at least partly explained by the accretion of atoms by grains under nonequilibrium conditions in diffuse clouds. With such an hypothesis one would expect the depletion to increase in the densest clouds, an assertion possibly supported by observations (see Section 5.2). Whether or not we have a precise explanation for the pattern seen in Figure 3a, it is clear that these data provide important indirect information about the dust. The large depletions for Si, Mg, Fe, Cr, Ti, Ca, Ni, and Al imply that these species are nearly completely tied up in the dust and any grain theory must include them. In contrast, S and Zn are not greatly depleted and probably are an un-important grain constituent. On the basis of the exceedingly high depletions for some of these elements (10^3 to 10^4), it is apparent that the processes that remove these elements from the gas phase are much more efficient than those processes that convert the same solids back into gaseous matter.

For the low reddening line of sight less depletion is usually recorded. In Figure 3b the correlation between depletion and condensation temperature is weak. For other low reddening lines of sight, reasonable correlations are found (e.g. λ Sco; York 1975).

5.2 STUDIES OF A LIMITED NUMBER OF ELEMENTS TOWARD MANY STARS

Figures 3a and b indicate a complex behavior in the depletion pattern from region to region in the Galaxy. Studies of this behavior can potentially provide valuable clues about the formation and destruction of dust grains. The classic Routly-Spitzer effect illustrates the kind of insights that can be gained from these studies. Routly & Spitzer (1952) noted that the Na I to Ca II column density ratio varied significantly with cloud velocity in the sense that N(Na I)/N(Ca II) is much smaller in the high velocity clouds. For a recent discussion of this effect see Siluk & Silk

(1974). It now seems well established that this abundance variation is the result of grain destruction in the high velocity clouds (Shull, York & Hobbs 1977). In this particular case Na is relatively undepleted while Ca is highly depleted and grain destruction of Ca-bearing grains returns a considerable amount of Ca to the gas phase and hence a smaller ratio of N(Na I) to N(Ca II) is observed. Similar effects have also been noted for Fe and Si when compared to S (Jenkins, Silk & Wallerstein 1976, Shull, York & Hobbs 1977). Thus, depletion studies can potentially provide information on the ease with which grains can be destroyed by interstellar shocks. For theoretical discussions of the destruction process see Shull (1977) and Barlow & Silk (1977).

Extensive survey measurements of elemental depletion toward many stars have been reported by Hobbs (1974, 1978) for Na, Ca, and K, by Stokes (1978) for Ti, and by Savage & Bohlin (1979) for Fe. Ca, Ti, and Fe exhibit large and variable depletions while Na and K exhibit at most a modest depletion with very little variability. The variability observed for Ca, Ti, and Fe amounts to about a factor of 100. However, the depletion of these three elements is reasonably well correlated (Stokes 1978, Savage & Bohlin 1979). From this one can probably conclude that grains bearing Ca, Ti, and Fe have roughly similar formation and/or destruction properties. However, detailed profile comparisons between Ca II and Ti II demonstrate that a one-to-one relation between the depletion variations is not present (Stokes 1978); hence, the Ca and Ti may be located in different grains. While the data are more uncertain, the measurements of de Boer & Lamers (1978) indicate that some of these comments for Ca, Ti, and Fe can also be extended to include Mn.

The question of whether the observed depletion depends on cloud parameters is of vital importance for establishing if accretion is a process that operates in diffuse clouds. Infrared measurements of the 3.07 μm "ice" feature in dense clouds show that accretion must be important in dense clouds and it is reasonable to expect similar processes to occur in the lower density diffuse clouds. The observational results on the dependence of depletion on cloud density are contradictory. A major difficulty is in estimating cloud density for lines of sight that contain a very inhomogeneous distribution of matter. Stokes (1978) used the column densities of Ca II and Ti II to estimate electron densities in 110 clouds, found that the electron densities were uncorrelated with depletion, and concluded that depletion is not a simple or unique function of local density. In contrast, Savage & Bohlin (1979) found that the interstellar Fe depletion correlates with several crude indicators of cloud density in the sense that the largest depletions are recorded in the densest clouds. The density indicators were average line-of-sight hydrogen density, the reddening

1979ARA&A...17...73S

per unit distance, and the fractional abundance of line-of-sight hydrogen in the molecular form. While the first two indicators are very approximate, an excellent correlation did hold up over nearly a three decade range in $n(\mathrm{HI} + \mathrm{H}_2)$ and $E(B-V)/r$. Unfortunately, the observed correlations do not necessarily imply that accretion is actually occurring in the denser regions since the correlations could equally well be explained by a destruction process that is more effective at low density.

6   Thermal Emission from Grains

Interstellar dust absorbs incident radiation and re-emits the energy in the IR. The intensity of the emitted 5–400 μm radiation provides clues as to the nature, temperature, and distribution of the dust, but the observational data require a considerably more complicated analysis than was originally believed. For instance, there is often a considerable variation in the radiation field incident upon the dust along the line of sight. Hence, some of the dust may be in a hot circumstellar shell, quite close to a star, while the rest may be in a cooler surrounding region. Furthermore, there is likely to be a wide range of grain sizes and a number of grain materials at any given point. Because of the dependence of the absorption and emission efficiencies on size, each grain size will assume a different temperature. A possible additional complication is that for very small grains (size <0.01 μm, say), the absorption of a single photon is enough to cause a large fluctuation in the temperature of the grain (Greenberg & Hong 1974a, Purcell 1976), so that the equilibrium temperature appropriate to the size has little significance. However, Drapatz & Michel (1977) find that defects in the grain structure will increase the specific heat and greatly reduce these temperature excursions. Without defects, a 0.01 μm silicate grain in the interstellar radiation field heats to about 20 K after the absorption of a photon, and quickly cools to 4 K. Its steady-state temperature, obtained from balancing average energy input and radiation loss rates, is about 12 K. A 0.1 μm silicate grain will have smaller fluctuations and be at about 8 K. In H I regions, graphite grains of size 0.05 μm are at about 35 K. Inside H II regions, graphite grains are at about 200 K and 0.1 μm silicate grains are at about 80 K. Rather elaborate models, based on assumptions about the sizes and materials in the grains, have been necessary to interpret the observations of both molecular clouds and H II regions (Scoville & Kwan 1976, Aannestad 1978).

6.1   EMISSION FROM GASEOUS NEBULAE   There is abundant evidence that dust is intimately mixed with the ionized gas in at least some giant, ordinary, and compact H II regions (see Panagia 1977 and Mezger &

Wink 1977 for reviews). This evidence is partly based on the spatial coincidence of the free-free radio continuum and IR radiation. Furthermore, there is so much radiation in the far IR ($\lambda > 25$ μm) that some energy must be supplied to the dust by hydrogen-ionizing radiation from the star (Panagia 1977, Emerson & Jennings 1978). The IR spectra of many diverse objects are very similar (Thronson & Harper 1979). The intensity I_ν peaks at about 70 μm but is broader than emission from dust with any reasonable optical properties at a single temperature. The peak intensity is lower than the Planck function intensity by substantial factors (~ 50) for optical H II regions, such as Orion and M 16, indicating that the sources are optically thin. For all sources, the emission is far brighter than the free-free emission would be, as extrapolated from the higher radio frequencies. The spectra of many objects decline in a similar way in the far-IR ($\lambda > 100$ μm) region, indicating that the grains' absorption efficiency (i.e. actual absorption cross section, divided by the geometrical cross section) decreases at least as fast as λ^{-1} or λ^{-2}. This decline is consistent either with disordered silicates (Day 1976), which are necessary to explain the shape of the 9.7 μm feature, or with graphite. It is likely that the decline of the far-IR spectrum is also consistent with emission from amorphous carbon. IC 418, an otherwise fairly typical planetary nebula, has an unusually narrow far-IR spectrum, which drops as λ^{-3} at long wavelengths (Moseley 1979).

Models (e.g. Natta & Panagia 1976) show that it is not possible to derive the total mass of the grains unless far-IR ($\lambda > 25$ μm) observations are available. Large grains, containing most of the mass, absorb only a small fraction of the stellar energy and radiate it only in the far-IR because they are cold. Thus, one must view claims of dust deficiencies in H II regions with caution if the observations do not extend to ~ 100 μm.

The rate of formation of planetary nebulae indicates that they are a significant source of mass input into the interstellar medium. Furthermore, their spectra show continuous IR radiation from heated dust, as well as some narrower emission features, which probably arise from the dust. Dust in planetary nebulae has been reviewed by Balick (1978) and Mathis (1978). New observations have been reported by Moseley (1979), Willner et al. (1978), and McCarthy, Forrest & Houck (1978). The continua peak at shorter wavelengths (~ 30 μm) than in H II regions, indicating warmer grains. As for H II regions, at long wavelengths the absorption efficiency usually drops as λ^{-1} to λ^{-2}.

The 9.7 μm silicate band is not seen in any planetary nebula. Since the C/O abundance ratio in planetaries is significantly greater than unity (Torres-Peimbert & Peimbert 1977, Shields 1978), one would expect the condensates to be SiC and graphite, or possibly amorphous carbon,

rather than silicates. Thus, the lack of the 9.7 μm band in planetaries further strengthens its identification with silicates. The broad far-IR emissivity of the planetary is, therefore, presumably caused by graphite or amorphous carbon.

There are several unidentified IR features found in a wide variety of objects, including several H II regions, several planetary nebulae, the galaxies M82 and NGC 253, and some stars with dusty shells (see Merrill 1977 for a review and references). The features occur at 3.3, 6.2, 7.7, 8.7, and 11.3 μm. The 11.3 μm feature is usually narrower than the 11.2 μm emission indentified with SiC in carbon stars (Treffers & Cohen 1974). The identification of the 11.3 μm feature with carbonates is appealing, but can be ruled out by the lack of the 7 μm and 45 μm features, which should be even stronger but are not observed (McCarthy, Forrest & Houck 1978, Russell, Soifer & Willner 1978). The 3.3 μm feature, usually with a wing at 3.4 μm, is apparently continuous at a resolution of $\lambda/\Delta\lambda \sim 3000$ (H. Smith, quoted in an extensive discussion of the feature by Russell, Soifer & Merrill 1977) and is apparently not caused by molecular bands. However, the profile does appear to be different in the planetary nebulae NGC 7027, NGC 6572, and IC 418 (Willner et al. 1978), and is uncorrelated with the excitation of the nebula. IC 418 and NGC 6572 have 11.2 μm features similar to those attributed to SiC in carbon stars, but even broader; possibly the SiC grains are very large.

The Galactic plane has been detected in the 100 μm spectral region (Rouan et al. 1977, Low et al. 1977, Serra et al. 1978). There is diffuse radiation not associated with specific sources. The emission may come mainly from dust in the vicinity of hot young stars. The most direct implication is that the rate of star formation per mass of gas is larger in the inner regions of the Galaxy than it is near the sun.

6.2 EMISSION FROM STARS AND NOVAE   In this section we briefly consider stars that are expelling dust into the interstellar medium. Cool stars are discussed in an excellent review by Merrill (1977), and many of the observations are in Forrest, Gillett & Stein (1975) and Merrill & Stein (1976a,b,c). Briefly, M stars (O/C > 1) show the 9.7 μm silicate band in either emission or absorption, depending upon the extent of the circumstellar dust shell. When a large emission feature is observed, the profile is very similar to the emission found in the Orion Nebula near the Trapezium. The 18 μm silicate band is also in absorption in some cases (Forrest et al. 1978), but is partially filled in by emission. Models (Jones & Merrill 1976) are required for a detailed interpretation, but there is little doubt that M stars are injecting silicate grains into the interstellar medium.

By contrast, carbon stars do not show the 9.7 μm emission feature, but rather 10–12 μm emission of SiC (Treffers & Cohen 1974). This emission is much wider than the unidentified 11.3 μm feature of planetary nebulae. Carbon stars also show a featureless component with a broad far-IR emissivity, presumably from graphite or possibly amorphous carbon.

Most early-type stars do not show IR excesses that clearly indicate grain emission. A number of exceptions (Allen 1973) include several Herbig Ae/Be stars and some peculiar Ae, Be objects. An extreme case is HD 45677, which exhibits a featureless IR emission spectrum resembling that found for carbon stars. The measurements of the 2200 Å feature for this star were discussed in Section 1.2. A number of WC7–WC9 stars (Gehrz & Hackwell 1974, Cohen, Barlow & Kuhi 1975) show the broad,

Table 3 Spectroscopic features produced by interstellar and/or circumstellar dust

Feature	Where seen[a]	Where not seen[a,b]	Common explanation
Rapid extinction rise for $\lambda < 1300$ Å	DC	—	small interstellar grains
2200 Å feature	DC,CS	—	graphite
Diffuse interstellar features[c]	DC	CS	—
Very broad structure in the visual	DC	—	magnetite?
3.07 μm	MC	DC,CSC,CSO,DN	H_2O and/or NH_3 ice
9.7 μm (sometimes with 18 μm)	DC,MC,CSO,DN,C	N,CSC,PN	silicates
11.2 μm	CSC	—	silicon carbide
Unidentified IR features at 3.3, 3.4, 6.2, 7.7, 8.7, and 11.3 μm[c]	CS,DN	DC	—

[a] C   comets
CS   circumstellar shells (composition unknown)
CSC   circumstellar shells (carbon-rich)
CSO   circumstellar shells (oxygen-rich)
DN   diffuse nebulae
DC   diffuse clouds
MC   molecular clouds
N   novae (presumably carbon-rich)
PN   planetary nebulae (carbon-rich)
[b] Entries in this column imply that the feature or features have been looked for but not detected.
[c] Some of these may have a molecular origin.

featureless emission expected from graphite, with no trace of silicate or silicon carbide features.

Some novae also form dust grains. References are given and the subject is reviewed by Gallagher & Starrfield (1978). The grain formation is related to the speed class, with the slow novae being favored. There is no 9.7 μm silicate emission. Theoretical models for novae suggest that $C/O > 1$ in order to produce the explosion. The implication, then, is that novae are producing carbon grains.

Table 3 summarizes the objects in which various features are found, as well as the objects in which they have not been found after a careful search. The table points out that the 9.7 μm silicate feature has been seen in several comets (see Ney 1977 for a review). Snow (1973) notes that the diffuse interstellar features are not formed in circumstellar dust shells. References to the other entries are contained in the text.

7   Diffuse Interstellar Features

The diffuse interstellar features (sometimes called diffuse interstellar bands) represent one of the longest standing unsolved problems in all of spectroscopy. This is unfortunate since these features probably contain a multitude of clues about the composition and physical nature of interstellar dust. While it is not established that these features have a solid-state origin, it is worth noting that the diffuse features are seen toward stars behind diffuse interstellar clouds, and thus far only simple diatomic molecules have been detected along such lines of sight. Therefore, explanations that involve polyatomic molecules would appear untenable. However, for arguments favoring a molecular origin see Smith, Snow & York (1977).

The diffuse features are numerous. Herbig (1975), in his extensive and important investigation covering the wavelength region 4400–6850 Å, detected 39 features of certain or probable interstellar origin with full widths at half intensity ranging from about 1 Å to about 20 Å. Recently, the study of these features has been extended to longer and shorter wavelengths. Sanner, Snell & van den Bout (1978) present results for several additional features between 6500 and 8900 Å. Snow, York & Resnick (1977) possibly detected an ultraviolet feature at 1416 Å in a search between 1114 and 1450 Å. However, Savage (1975) finds no evidence for diffuse features between 2000 and 3600 Å with the exception of the 2200 Å feature.

A compilation of diffuse feature measurements is provided by Snow, York & Welty (1977), where measurements for four features are collected and reduced statistically to a common measurement system. Much of the effort in studying the diffuse features has gone into investigating the

correlations of diffuse feature strengths with various interstellar quantities such as $E(B-V)$ and other reddening indicators. The principal results of these correlation studies are summarized in articles by Herbig (1975), Smith, Snow & York (1977), Schmidt (1978), and Sneden et al. (1978). Correlation studies may have been overemphasized and studies that might provide more useful *direct* physical information about the features have been neglected.

Van de Hulst (1957) first discussed the asymmetric profiles expected for the diffuse features if they are produced by scattering and absorption in interstellar grains. The degree of asymmetry depends on the particle optical constants and size. Therefore, profile measurements can potentially provide diagnostic information on the sizes of the diffuse feature carriers. For more recent theoretical discussions of diffuse feature profiles, see Bromage (1972), Savage (1976), and Purcell & Shapiro (1977). The early attempts to measure diffuse feature profiles concentrated on the broad features in the blue and the results were often contradictory. The most modern measurements for $\lambda 4430$ yield symmetric profiles (Danks & Lambert 1975, Martin & Angel 1975). For the broad features, reliable profile measurements are difficult to make because of the problem of establishing an accurate continuum level over a large wavelength span. This problem is further aggravated by the fact that numerous stellar lines occur in the general vicinity of the strongest broad diffuse features such as the feature near 4430 Å. Higher precision profile measurements can be obtained for the narrower features in the red. This is because these features are deeper and the continuum placement is easier. However, for the very narrow features, Doppler smearing due to the existence of multiple clouds can present a problem. High resolution profiles for features at 5780, 5797, 6379, and 6614 Å have been reported by Savage (1976), Danks & Lambert (1976), and Welter & Savage (1977). Asymmetries were found for the features at 5780, 5797, and 6614 Å. However, the feature at 6379 Å was symmetrical. From a detailed analysis of the observed profiles for the features at 5780, 6379, and 6614 Å, Savage (1976) and Welter & Savage (1977) conclude that a solid-state origin is the most likely explanation for these three features. It is also noted that the processes of autoionization and preionization, at least in the simple cases, could be ruled out since the profiles do not appear to have the required broad Lorentzian wings. An extension of this profile work using detectors capable of producing spectra with high signal to noise appears desirable. Perhaps new studies could provide a convincing demonstration of intrinsic profile variability from star to star which could more readily be explained by theories involving interstellar solids than by molecular absorption.

Studies of the polarization characteristics across the diffuse features are also an important way of establishing their origin (Martin & Angel 1974, Greenberg & Hong 1974b). High quality measurements now exist for the features at 4430, 5780, and 6284 Å (Martin & Angel 1974, 1975, Fahlman & Walker 1975) and the results all imply no polarization variations across the bands. These studies imply that the three features are not formed in those grains that produce the visible interstellar polarization. While this seems to favor the molecular explanation, the absence of a large polarization change across the 2200 Å feature (see Section 4) implies that nonpolarizing grain components do exist in the interstellar medium.

The ultimate identification of the diffuse features will probably come through laboratory investigations of the spectra and solids at low temperature. Unfortunately, very little laboratory work on plausible solids is currently being pursued.

8   Composition of Grains

In this section, we first discuss a possible picture of the composition and origin of interstellar grains, somewhat along the lines of Field (1978). We then discuss some of the problems associated with this picture and some alternative ideas. The growth of grains has been reviewed by Salpeter (1977) and will not be considered here.

As we discussed in Section 6, it is widely accepted that silicates are being injected by oxygen-rich M stars into the interstellar medium. Carbon-rich objects (primarily planetary nebulae, but also carbon stars and presumably novae) are also losing mass and injecting grains into the interstellar medium, probably both SiC and graphite or amorphous carbon. Small uncoated graphite grains have an extinction bump near 2200 Å, although the exact wavelength at which it occurs depends on the condition of the material and upon the shape and size of the particles. Graphite can also be abundant enough to produce the bump, while silicates can not if the absorption is classical. If this picture is right, the lack of polarization of the bump (which needs further observational confirmation) indicates that small graphite particles do not polarize, probably because they are not aligned. Similarly, the wavelength dependences of the circular and linear optical polarization militate against moderate-sized graphite particles as producers of the polarization and suggest that a dielectric, such as a silicate, is responsible. Furthermore, the 9.7 μm silicate feature is highly polarized in some objects, clearly indicating that silicates can be aligned. A power-law particle size distribution ($n[a] \propto a^{-3.5}$) of uncoated graphite and silicates produces a very good fit to the observed extinction (Mathis, Rumpl & Nordsieck 1977), while other substances

suggests that the bump arises from the plasma oscillations of electrons in very small dielectric particles ($\lesssim 30$ Å, or $\lesssim 1000$ atoms in each), while in this theory the 9.7 μm feature arises from the plasma oscillations of the ions in particles of sizes $\lesssim 0.3$ μm. The extinction at other wavelengths arises from off-resonance absorption of both ions and electrons. There have been many other suggestions. A few include lattice defects in small crystals (Drapatz & Michel 1976), and small silicate grains, which would apparently require an abundance of silicon greater than the solar value (Huffman & Stapp 1971).

ACKNOWLEDGMENTS

Literature Cited

Aannestad, P. A. 1978. *Ap. J.* 220:538
Aannestad, P. A., Purcell, E. M. 1973. *Ann. Rev. Astron. Astrophys.* 11:309
Allen, D. A. 1973. *MNRAS* 161:145
Andriesse, C. D. 1977. *Vistas Astron.* 21:107
Andriesse, C. D., Piersma, T. R., Witt, A. N. 1977. *Astron. Astrophys.* 54:841
Baldwin, J. A. 1977. *MNRAS* 178:67
Balick, B. 1975. *Ap. J.* 201:705
Balick, B. 1978. In *Planetary Nebulae, Theory and Observations. IAU Symp. 76,* ed. Y. Terzian, p. 275. Dordrecht: Reidel
Barlow, M. J., Silk, J. 1977. *Ap. J. Lett.* 211:L83
Becklin, E. E., Matthews, K., Neugebauer, G., Willner, S. P. 1978. *Ap. J.* 220:831
Becklin, E. E., Neugebauer, G. 1967. *Ap. J.* 147:799
Bless, R. C., Savage, B. D. 1972. *Ap. J.* 171:293
Boesgaard, A. M., Praderie, F., Leckrone, D. S., Faraggiana, R., Hack, M. 1974. *Ap. J. Lett.* 194:L143
Bohlin, R. C., Savage, B. D., Drake, J. F. 1978. *Ap. J.* 224:132
Bromage, G. E. 1972. *Astrophys. Space Sci.* 15:426
Brown, R. L., Lockman, F. J., Knapp, G. R. 1978. *Ann. Rev. Astron. Astrophys.* 16:445
Burstein, D., Heiles, C. 1978. *Ap. J.* 225:40
Capps, R. W., Knacke, R. F. 1976. *Ap. J.* 210:76
Carrasco, L., Strom, S. E., Strom, K. M. 1973. *Ap. J.* 182:95
Carruthers, G. R., Opal, C. B. 1977. *Ap. J. Lett.* 212:L27

Chaisson, E. J., Lichten, S. M., Rodriguez, L. F. 1978. *Ap. J.* 221:810
Chylek, P., Grams, G. W., Pinnick, R. G. 1976. *Science* 193:480
Code, A. D., Davis, J., Bless, R. C., Hanbury Brown, R. 1976. *Ap. J.* 203:417
Cohen, M., Barlow, M. J., Kuhi, L. V. 1975. *Astron. Astrophys.* 40:291
Coyne, G. V., Gehrels, T., Serkowski, K. 1974. *Astron. J.* 79:581
Danks, A. C., Lambert, D. L. 1975. *Astron. Astrophys.* 41:455
Danks, A. C., Lambert, D. L. 1976. *MNRAS* 174:571
Day, K. L. 1976. *Ap. J.* 210:614
de Boer, K. S. 1979. *Ap. J.* 229:132
de Boer, K. S., Lamers, H. J. G. L. M. 1978. *Astron. Astrophys.* 69:327
de Jong, T. 1976. *Mem. Soc. Astron. Italiana* 45:189
Dorschner, J., Friedemann, C., Gürtler, J. 1977. *Astron. Astrophys.* 58:201
Drapatz, S., Michel, K. W. 1976. *Mitt. Astron. Ges.* 40:187
Drapatz, S., Michel, K. W. 1977. *Astron. Astrophys.* 56:353
Duley, W. W. 1976. *Astrophys. Space Sci.* 45:253
Duley, W. W., Millar, T. J. 1978. *Ap. J.* 220:124
Dyck, H. M., Beichman, C. A. 1974. *Ap. J.* 194:57
Dyck, H. M., Capps, R. W. 1978. *Ap. J. Lett.* 220:L49
Dyck, H. M., Jones, T. J. 1978. *Astron. J.* 83:594

Egan, W. G., Hilgeman, T. 1978. *Nature* 273:369

Elsässer, H., Fechtig, H., eds. 1976. *Interplanetary Dust and Zodiacal Light, IAU Colloq. 31.* Berlin: Springer. 493 pp.

Emerson, J. P., Jennings, R. E. 1978. *Astron. Astrophys.* 69:129

Fahlman, G. G., Walker, G. A. H. 1975. *Ap. J.* 200:22

Field, G. B. 1974. *Ap. J.* 187:453

Field, G. B. 1978. In *Planetary Nebulae, Theory and Observations, IAU Symp. 76,* ed. Y. Terzian, p. 367. Dordrecht: Reidel

Field, G. B., Cameron, A. G. W., eds. 1975. *The Dusty Universe.* New York: Neale Watson. 323 pp.

FitzGerald, M. P. 1968. *Astron. J.* 73:983

FitzGerald, M. P., Stephens, T. C., Witt, A. N. 1976. *Ap. J.* 208:709

Forrest, W. J., Gillett, F. C., Houck, J. R., McCarthy, J. F., Merrill, K. M., Pipher, J. L., Puetter, R. C., Russell, R. W., Soifer, B. T., Willner, S. P. 1978. *Ap. J.* 219:114

Forrest, W. J., Gillett, F. C., Stein, W. A. 1975. *Ap. J.* 195:423

Forrest, W. J., Houck, J. R., Reed, R. A. 1976. *Ap. J. Lett.* 208:L133

Forrest, W. J., Soifer, B. T. 1976. *Ap. J. Lett.* 208:L129

Frogel, J. A., Persson, S. E., Aaronson, M. 1977. *Ap. J.* 213:723

Gallagher, J. S., Starrfield, S. 1978. *Ann. Rev. Astron. Astrophys.* 16:171

Gehrels, T. 1974. *Astron. J.* 79:590

Gehrz, R. D., Hackwell, J. A. 1974. *Ap. J.* 194:619

Gillett, F. C., Forrest, W. J. 1973. *Ap. J.* 179:483

Gillett, F. C., Forrest, W. J., Merrill, K. M., Capps, R. W., Soifer, B. T. 1975a. *Ap. J.* 200:609

Gillett, F. C., Jones, T. W., Merrill, K. M., Stein, W. A. 1975b. *Astron. Astrophys.* 45:77

Gilra, D. P. 1971. *Nature* 220:237

Greenberg, J. M. 1974. *Ap. J. Lett.* 189:L81

Greenberg, J. M. 1976. *Astrophys. Space Sci.* 39:9

Greenberg, J. M. 1978. In *Cosmic Dust,* ed. J. A. M. McDonnell, p. 187. New York: Wiley

Greenberg, J. M., Hong, S. S. 1974a. In *Galactic Radio Astronomy, IAU Symp. 60,* ed. F. J. Kerr, S. C. Simonson III, p. 155. Dordrecht: Reidel

Greenberg, J. M., Hong, S. S. 1974b. In *Planets, Stars and Nebulae Studied with Photopolarimetry,* ed. T. Gehrels. p. 916. Tucson: Univ. Arizona Press

Greenberg, J. M., van de Hulst, H. C., eds. 1973. *Interstellar Dust and Related Topics, IAU Symp. 52.* Dordrecht: Reidel

Hayes, D. S., Greenberg, J. M., Mavko, G. E., Radick, R. R., Rex, K. H. 1973. In *Interstellar Dust and Related Topics, IAU Symp. 52,* ed. J. M. Greenberg, H. C. van de Hulst, p. 83. Dordrecht: Reidel

Heiles, C., Jenkins, E. B. 1976. *Astron. Astrophys.* 46:333

Henry, R. C. 1977. *Ap. J. Suppl.* 33:451

Henry, R. C., Swandic, J. R., Schulman, S. D., Fritz, G. 1977. *Ap. J.* 212:707

Henyey, L. G., Greenstein, J. L. 1941. *Ap. J.* 93:70

Herbig, G. H. 1975. *Ap. J.* 196:129

Hobbs, L. M. 1974. *Ap. J.* 191:381

Hobbs, L. M. 1978. *Ap. J. Suppl.* 38:129

Hoyle, F., Wickramasinghe, N. C. 1977. *Nature* 268:610

Hudson, H. S., Soifer, B. T. 1976. *Ap. J.* 206:100

Huffman, D. R. 1977. *Adv. Phys.* 26:129

Huffman, D. R., Stapp, J. L. 1971. *Nature Phys. Sci.* 229:45

Isobe, S. 1977. In *Topics in Interstellar Matter,* ed. H. van Woerden, p. 61. Dordrecht: Reidel

Jenkins, E. B. 1976. In *The Structure and Content of the Galaxy and Galactic Gamma Rays,* ed. C. E. Fichtel, F. W. Stecker, p. 239. Greenbelt: NASA

Jenkins, E. B., Savage, B. D. 1974. *Ap. J.* 187:243

Jenkins, E. B., Silk, J., Wallerstein, G. 1976. *Ap. J. Suppl.* 32:681

Johnson, H. L. 1968. In *Nebulae and Interstellar Matter,* ed. B. M. Middlehurst, L. H. Aller, p. 167. Chicago: Univ. Chicago Press

Johnson, H. L. 1977. *Rev. Mex. Astron. Astrof.* 2:175

Jones, T. W., Merrill, K. M. 1976. *Ap. J.* 209:509

Jura, M. 1977. *Ap. J.* 218:749

Jura, M., York, D. G. 1978. *Ap. J.* 219:861

Kattawar, G. W. 1975. *J. Quant. Spectrosc. Radiat. Transfer* 15:839

Knacke, R. F., Capps, R. W. 1977. *Ap. J.* 216:271

Knapp, G. R., Kerr, F. J. 1974. *Astron. Astrophys.* 35:361

Koornneef, J. 1978a. *Astron. Astrophys.* 64:179

Koornneef, J. 1978b. *Astron. Astrophys.* 68:139

Krätschmer, W., Huffman, D. R. 1979. Preprint

Lillie, C. F., Witt, A. N. 1976. *Ap. J.* 208:64

Low, F. J., Kurtz, R. F., Poteet, W. M., Nishimura, T. 1977. *Ap. J. Lett.* 214:L115

Lucke, P. B. 1978. *Astron. Astrophys.* 64:367

Lugger, P. M., York, D. G., Blanchard, T., Morton, D. C. 1978. *Ap. J.* 224:1059

Lynds, B. T. 1962. *Ap. J. Suppl.* 7:1

Lynds, B. T. 1965. *Ap. J. Suppl.* 12:163
Martin, P. G. 1972. *MNRAS* 159:179
Martin, P. G. 1974. *Ap. J.* 187:461
Martin, P. G. 1975. *Ap. J.* 201:373
Martin, P. G., Angel, J. R. P. 1974. *Ap. J.* 188:517
Martin, P. G., Angel, J. R. P. 1975. *Ap. J.* 195:379
Martin, P. G., Angel, J. R. P. 1976. *Ap. J.* 207:126
Martin, P. G., Campbell, B. 1976. *Ap. J.* 208:727
Mathis, J. S. 1978. In *Planetary Nebulae, Theory and Observations, IAU Symp. 76,* ed. Y. Terzian, p. 281. Dordrecht: Reidel
Mathis, J. S., Rumpl, W., Nordsieck, K. H. 1977. *Ap. J.* 217:425
Mattila, K. 1970. *Astron. Astrophys.* 9:53
Mattila, K. 1971. *Astron. Astrophys.* 15:292
McCarthy, J. F., Forrest, W. J., Houck, J. R. 1978. *Ap. J.* 224:109
McDonnell, J. A. M., ed. 1978. *Cosmic Dust.* New York: Wiley. 693 pp.
McMillan, R. S. 1978. *Ap. J.* 225:417
Merrill, K. M. 1977. In *The Interaction of Variable Stars with Their Environment, IAU Colloq. 42,* ed. R. Kippenhahn, J. Rahe, W. Strohmeier, p. 446. Bamberg: Remeis-Sternwarte
Merrill, K. M., Russell, R. W., Soifer, B. T. 1976. *Ap. J.* 207:763
Merrill, K. M., Stein, W. A. 1976a. *Publ. Astron. Soc. Pac.* 88:285
Merrill, K. M., Stein, W. A. 1976b. *Publ. Astron. Soc. Pac.* 88:294
Merrill, K. M., Stein, W. A. 1976c. *Publ. Astron. Soc. Pac.* 88:874
Mezger, P. G., Smith, L. F., Churchwell, E. B. 1974. *Astron. Astrophys.* 32:269
Mezger, P. G., Wink, J. E. 1977. *Infrared and Submillimeter Astronomy,* ed. G. G. Fazio, p. 55. Dordrecht: Reidel
Morgan, D. H., Nandy, K., Thompson, G. I. 1976. *MNRAS* 177:531
Morton, D. C. 1975. *Ap. J.* 197:85
Morton, D. C. 1978. *Ap. J.* 222:863
Morton, D. C., Hu, E. M. 1975. *Ap. J.* 202:638
Moseley, H. 1979. *Ap. J.* In press
Nachman, P., Hobbs, L. M. 1973. *Ap. J.* 182:481
Nandy, K., Thompson, G. I., Jamar, C., Monfils, A., Wilson, R. 1975. *Astron. Astrophys.* 44:195
Nandy, K., Thompson, G. I., Jamar, C., Monfils, A., Wilson, R. 1976. *Astron. Astrophys.* 51:63
Natta, A., Panagia, N. 1976. *Astron. Astrophys.* 50:191
Neugebauer, G., Becklin, E. E., Matthews, K., Wynn-Williams, C. G. 1978. *Ap. J.* 220:149

Ney, E. P. 1977. *Science* 195:541
Ney, E. P., Strecker, D. W., Gehrz, R. D. 1973. *Ap. J.* 180:807
Oort, J. H. 1977. *Ann. Rev. Astron. Astrophys.* 15:295
Panagia, N. 1977. In *Infrared and Submillimeter Astronomy,* ed. G. G. Fazio, p. 43. Dordrecht: Reidel
Panagia, N., Smith, L. F. 1978. *Astron. Astrophys.* 62:277
Peimbert, M., Torres-Peimbert, S. 1977. *MNRAS* 179:217
Penston, M. V., Hunter, J. K., O'Neill, A. 1975. *MNRAS* 171:219
Persson, S., Frogel, J. A., Aaronson, M. 1976. *Ap. J.* 208:753
Platt, J. R. 1956. *Ap. J.* 123:486
Purcell, E. M. 1976. *Ap. J.* 206:685
Purcell, E. M., Shapiro, P. R. 1977. *Ap. J.* 214:92
Roach, F. E., Megill, L. R. 1961. *Ap. J.* 133:228
Rouan, D., Lena, P. J., Puget, J. L., de Boer, K. S., Wijnbergen, J. J. 1977. *Ap. J. Lett.* 213:L35
Routly, P. M., Spitzer, L. 1952. *Ap. J.* 115:227
Russell, R. W., Soifer, B. T., Merrill, K. M. 1977. *Ap. J.* 213:66
Russell, R. W., Soifer, B. T., Willner, S. P. 1978. *Ap. J.* 220:568
Salpeter, E. E. 1977. *Ann. Rev. Astron. Astrophys.* 15:267
Sanner, F., Snell, R., van den Bout, P. 1978. *Ap. J.* 226:460
Sarazin, C. L. 1976. *Ap. J.* 208:323
Savage, B. D. 1975. *Ap. J.* 199:92
Savage, B. D. 1976. *Ap. J.* 205:122
Savage, B. D., Bohlin, R. C. 1978. *Bull. Am. Astron. Soc.* 10:445
Savage, B. D., Bohlin, R. C. 1979. *Ap. J.* 229:136
Savage, B. D., Bohlin, R. C., Drake, J. F., Budich, W. 1977. *Ap. J.* 216:291
Savage, B. D., Wesselius, P. R., Swings, J. P., Thé, P. S. 1978. *Ap. J.* 224:149
Schalén, C. 1975. *Astron. Astrophys.* 42:251
Schiffer, F. H., Mathis, J. S. 1974. *Ap. J.* 194:597
Schild, R. E. 1977. *Astron. J.* 82:337
Schmidt, E. G. 1978. *Ap. J.* 223:458
Schultz, G. V., Wiemer, W. 1975. *Astron. Astrophys.* 43:133
Scoville, N. Z., Kwan, J. 1976. *Ap. J.* 206:718
Serkowski, K., Mathewson, D. S., Ford, V. L. 1975. *Ap. J.* 196:261
Serra, G., Puget, J. L., Ryter, C. E., Wijnbergen, J. J. 1978. *Ap. J. Lett.* 222:L21
Shane, C. D., Wirtanen, C. A. 1967. *Lick Obs. Publ.* 22:1
Shapiro, P. R. 1975. *Ap. J.* 201:151
Shields, G. A. 1978. *Ap. J.* 219:559

Shull, J. M. 1977. *Ap. J.* 215:805
Shull, J. M., York, D. G., Hobbs, L. M. 1977. *Ap. J. Lett.* 211:L139
Siluk, R. S., Silk, J. 1974. *Ap. J.* 192:51
Smith, W. H., Snow, T. P., York, D. G. 1977. *Ap. J.* 218:124
Sneden, C., Gehrz, R. D., Hackwell, J. A., York, D. G., Snow, T. P. 1978. *Ap. J.* 223:168
Snow, T. P. 1973. *Publ. Astron. Soc. Pac.* 85:590
Snow, T. P. 1975. *Ap. J. Lett.* 202:L87
Snow, T. P. 1976. *Ap. J.* 204:759
Snow, T. P. 1977. *Ap. J.* 216:724
Snow, T. P., York, D. G. 1975. *Astrophys. Space Sci.* 34:19
Snow, T. P., York, D. G., Resnick, M. 1977. *Publ. Astron. Soc. Pac.* 89:758
Snow, T. P., York, D. G., Welty, D. E. 1977. *Astron. J.* 82:113
Soifer, B. T., Russell, R. W., Merrill, K. M. 1976. *Ap. J. Lett.* 207:L83
Spitzer, L. 1978. *Physical Processes in the Interstellar Medium.* New York: Wiley. 318 pp.
Spitzer, L., Jenkins, E. B. 1975. *Ann. Rev. Astron. Astrophys.* 13:133
Stein, W. A. 1975. *Publ. Astron. Soc. Pac.* 87:5
Stokes, G. M. 1978. *Ap. J. Suppl.* 36:115
Strömgren, B. 1972. *Q. J. R. Astron. Soc.* 13:153
Torres-Peimbert, S., Peimbert, M. 1977. *Rev. Mex. Astron. Astrof.* 2:181
Thronson, H., Harper, D. A. 1979. *Ap. J.* In press
Thum, C., Mezger, P. G., Pankonin, V., Schraml, J. 1978. *Astron. Astrophys.* 64:L17
Treffers, R., Cohen, M. 1974. *Ap. J.* 188:545
van de Hulst, H. C. 1957. *Light Scattering by Small Particles.* New York: Wiley. 470 pp.
van Duinen, J. R., Wu, C.-C., Kester, D. 1976. *Department of Space Research Groningen Internal Note,* ROG NR 76-4
Watson, W. D., Salpeter, E. E. 1972. *Ap. J.* 174:321
Welter, G. L., Savage, B. D. 1977. *Ap. J.* 215:788

Wesson, P. S. 1974. *Space Sci. Rev.* 15:469
Whiteoak, J. B. 1966. *Ap. J.* 144:305
Whittet, D. C. B., van Breda, I. G. 1975. *Astrophys. Space Sci.* 38:L3
Whittet, D. C. B., van Breda, I. G. 1978. *Astron. Astrophys.* 66:57
Whittet, D. C. B., van Breda, I. G., Glass, I. S. 1976. *MNRAS* 177:625
Wickramasinghe, N. C., Morgan, D. H., eds. 1976. *Solid State Astrophysics, Astrophys. Space Sci. Library Vol. 55.* Dordrecht: Reidel. 314 pp. Also in *Astrophys. Space Sci.* 34:1 (1975)
Wickramasinghe, N. C., Nandy, K. 1972. *Rep. Prog. Phys.* 35:157
Willis, A. J., Wilson, R. 1975. *Astron. Astrophys.* 44:205
Willis, A. J., Wilson, R. 1977. *Astron. Astrophys.* 59:133
Willner, S. P. 1976. *Ap. J.* 206:728
Willner, S. P. 1977. *Ap. J.* 214:706
Willner, S. P., Jones, B., Puetter, R. C., Russell, R. W., Soifer, B. T. 1978. Preprint
Withbroe, G. L. 1971. In *The Menzel Symposium, NBS Spec. Pub. 353,* ed. K. B. Gebbie. Washington: NBS
Witt, A. N. 1968. *Ap. J.* 152:59
Witt, A. N. 1977. *Publ. Astron. Soc. Pac.* 89:750
Witt, A. N., Johnson, M. W. 1973. *Ap. J.* 181:363
Witt, A. N., Lillie, C. F. 1978. *Ap. J.* 222:909
Wu, C.-C. 1977a. *Ap. J. Lett.* 217:L117
Wu, C.-C. 1977b. *Bull. Am. Astron. Soc.* 9:296
Wynn-Williams, C. G., Becklin, E. E. 1974. *Publ. Astron. Soc. Pac.* 86:5
York, D. G. 1975. *Ap. J. Lett.* 196:L103
York, D. G., Drake, J. F., Jenkins, E. B., Morton, D. C., Rogerson, J. B., Spitzer, L. 1973. *Ap. J. Lett.* 182:L1
Zeippen, C. J., Seaton, M. J., Morton, D. C. 1977. *MNRAS* 181:527
Zerull, R. 1976. In *Interplanetary Dust and Zodiacal Light, IAU Colloq. 31,* ed. H. Elsasser, H. Fechtig, p. 130. Berlin: Springer